



Simulating the Misting of Lubricant in the Piston Assembly of an Automotive Gasoline Engine: The Effect of Viscosity Modifiers and Other Key Lubricant Components

Christopher J. Dyson¹ · Martin Priest² · Peter M. Lee³

Received: 17 January 2022 / Accepted: 21 March 2022
© The Author(s) 2022

Abstract

The presence of lubricant droplets in the gas that flows through the piston assembly and crankcase of an internal combustion engine (generically termed *oil misting*) has important implications for performance, particularly lubricant supply to the upper piston assembly, oil consumption and lubricant degradation. A significant source of these droplets is thought to be oil shearing and blow-through by blow-by gas flows in the piston assembly. An experimental rig was developed to simulate the high velocity gas and lubricant film interactions at a top piston ring gap where the flow conditions are most severe. Flows of lubricant droplets were produced and characterised in terms of the proportion of the oil flow that formed droplets in the gas flow and the size distribution of the droplets produced. Considering various aspects of a commercial automotive crankcase formulation, the effect of lubricant viscosity was found to be particularly important. Of the lubricant additives evaluated, viscosity modifiers were found to have the greatest effect on the tendency to form droplets: Detailed study on a range of viscosity modifiers identified that the influence of their molecular architectures on viscoelasticity was the key mechanism.

Keywords Crankcase lubricant · Droplet formation · Misting · Lubricant additives · Viscosity modifiers · Viscosity index improvers

1 Introduction

The lubrication of the piston assembly in an automotive engine has been studied in great detail due to its importance to the performance of an engine. For instance, Mufti et al. showed that between 33 and 44% of engine friction can be attributed to the piston assembly [1]. Tung et al. gave piston assembly friction as 44% of total engine friction, translating to approximately 5% of engine power usage [2]. Therefore, the effective lubricant supply to the piston assembly, particularly the upper piston rings where the tribological environment is most harsh, is a key factor in engine system design. Droplets of oil entering the combustion chamber are causes

of low speed pre-ignition (LSPI) in modern high power density, turbocharged engines [3–7]. Also, it has been shown that 80% of oil consumption can be attributed to lubricant flow paths through the piston assembly [8], which has a significant effect on exhaust emissions. Furthermore, based on the work of Yasutomi et al., it has been shown that the high temperatures, high shear stresses and exposure to hot air, fuel and combustion products in the piston assembly produces the most rapid rate and greatest source of lubricant degradation in the engine [9].

Much research over the years has established several key lubricant transport mechanisms, Fig. 1. These are:

- **Scraping** [10–18]
- **Evaporation** [10, 13, 18–23]
- **Ring Pumping** [10, 11, 13, 24, 25]
- **Inertia** [10, 11, 13, 18, 24, 26, 27]
- **Dragging by Blow-By Gas** [10, 18, 28–33]. Interfacial shear from blow-by gas over the surface of oil films causes the lubricant film to move in the predominant direction of gas flow: Circumferentially around the piston lands and through the ring gaps. When the ring gaps are

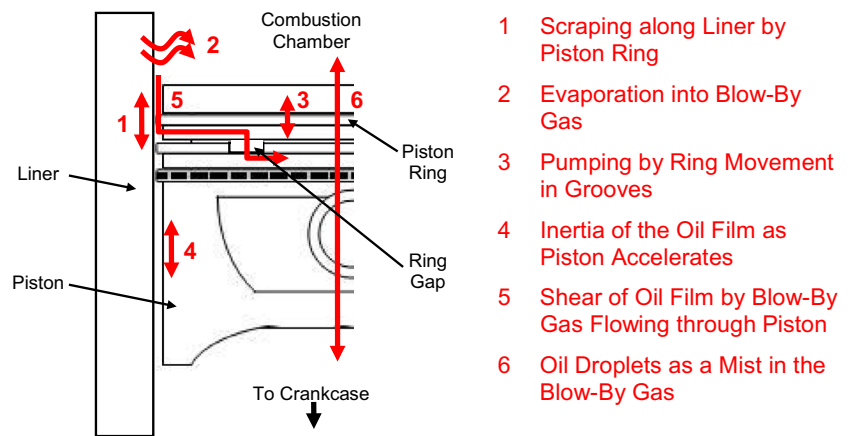
✉ Martin Priest
m.priest@bradford.ac.uk

¹ Formerly of School of Mechanical Engineering, University of Leeds, Leeds, UK

² Faculty of Engineering and Informatics, University of Bradford, Leeds, UK

³ Southwest Research Institute, San Antonio, TX, USA

Fig. 1 Lubricant transport mechanisms in the piston assembly of a fired automotive engine



circumferentially opposite on the piston (180° apart), the large area of lubricant film on the predominant gas flow path but gas flow rates are relatively low. When the ring gaps are vertically aligned (0° apart circumferentially), blow-by flow rate is high but lubricant flow rate by this mechanism is low. Thirouard et al. [15] found that the maximum lubricant flow rate is at an intermediate angle. These and other studies [34, 35] showed that relative ring gap position influences more than absolute position.

- **Ring Lift and Flutter** [25]. The flow of gas through the ring groove, behind the ring, causes the lubricant in the ring groove to be rapidly evacuated, predominantly, in the direction of the gas flow. This can cause high levels of lubricant consumption, particularly when the flow of gas is upwards into the combustion chamber (reverse blow-by).
- **Misting** [10–12, 15, 18, 36]. Lubricant droplets are carried by the gas flow until they are deposited or until they leave the engine.

Generally termed misting, although referring to droplets typical of aerosols, mists and sprays, the presence of droplets in the gas flow of the piston assembly and crankcase has been discussed for many years, from the perspectives of oil consumption and lubricant transport. However, little of this has been previously understood. It is thought that droplets can be produced in several ways: Firstly, the high gas flow rates and shear over the lubricant film around the ring gaps might produce droplets [15, 28].

Secondly, droplets may form by air flow through the ring and liner interface, particularly when significant bore distortion is seen: The lubricant film is ‘blown through’ when the pressure differential across the ring is greater than the interface oil film can support [37].

Thirdly, a similar effect has been observed with certain designs of oil control ring, lubricant pockets are ‘blown through’ [24]: This might also occur in other areas where

oil can accumulate in a potential gas flow path such as oil drain holes and the piston skirt.

Fourthly, oil vapour generated in the piston assembly condenses into droplets when it reaches cools in the crankcase. Condensed droplets are typically in the order of 10^{-7} – 10^{-6} m in diameter, whereas mechanically formed droplets are in the order of 10^{-5} – 10^{-4} m [38].

The presence of lubricant droplets in the crankcase has been associated with deposit and varnish on turbochargers and intake components if exhaust gas is recirculated [39], affecting key systems in modern engines. Oil transport mechanisms have been shown to be affected by transient engine conditions [24], where oil can accumulate and dissipate rapidly, so the frequent start/stop cycles in hybrid engines [40] may contribute to the influence of droplets on these effects.

The aim of this investigation was to simulate the oil mist formation mechanisms thought to occur at the piston ring gaps in a controlled laboratory environment, where the influence of individual parameters and their interactions could be systematically and rigorously investigated. Bespoke apparatus was designed and built for this purpose. Stage 1 of the research investigated the mist forming tendency of the relevant components of a commercial lubricant to determine which had the greatest effect on the mist formation process. This led to a more detailed study of the influence of viscosity modifiers, Stage 2.

2 Methodology

2.1 Apparatus

The apparatus developed for this study utilised a venturi mist generator to produce an oil mist flow. This flow was measured using a particle sizer, and by weighing the oil in various flows before and after the test, Fig. 2.

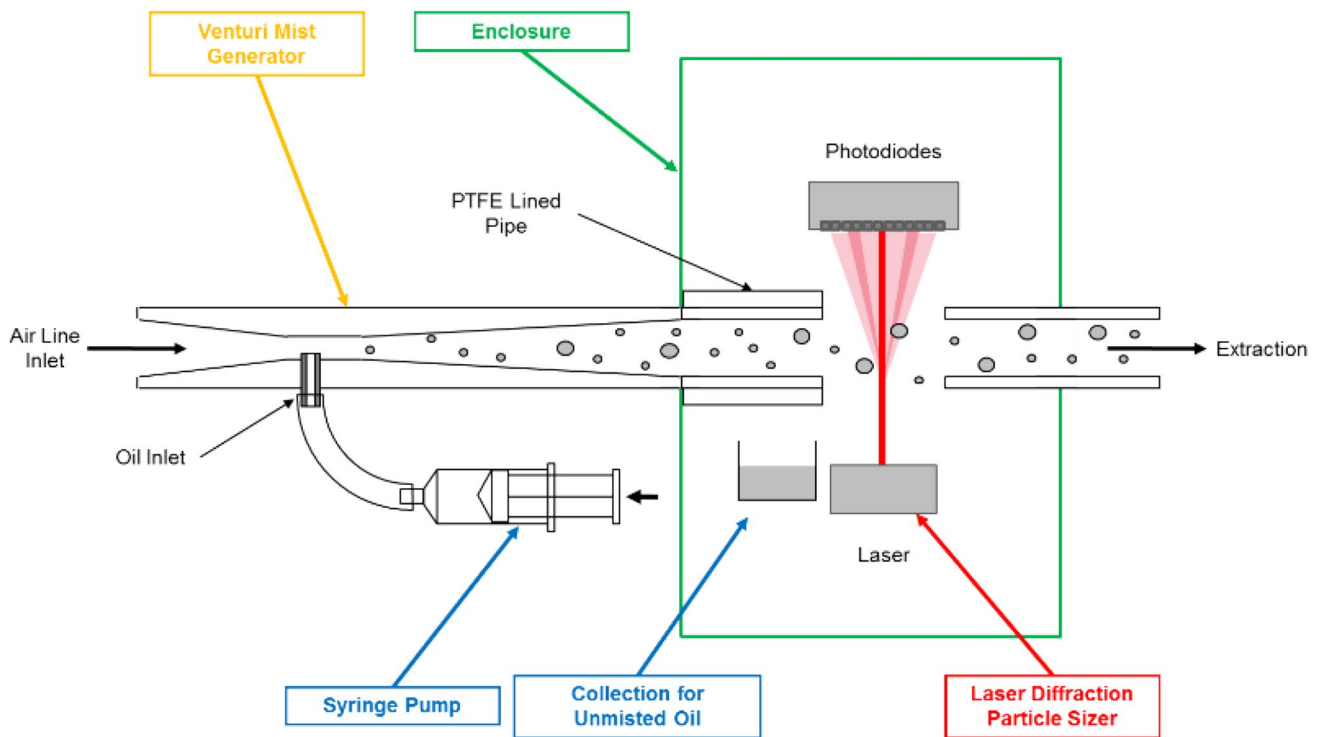


Fig. 2 Schematic of mist generator and measurement equipment

Table 1 Comparison of venturi mist generator flow parameters with those modelled in an engine

| Parameter | Top piston ring gap after Gamble et al. [12] | Venturi mist generator |
|--|--|------------------------|
| Peak air inlet gauge pressure ($\times 10^6$ Pa) | 3.94 | 0.15 |
| Peak throat gauge pressure ($\times 10^6$ Pa) | 3.94 | 0.053 |
| Peak air mass flow rate ($10^{-3} \text{ m}^3\text{s}^{-1}$) | 1.01 | 1.54 |
| Peak air velocity (ms^{-1}) | 438 | 300 |
| Mach number | 0.91 | 1 |
| Expansion ratio | 3.42–13.23 | 11.67 |
| Gas temperature ($^{\circ}\text{C}$) | ≈ 200 | 20 |
| Oil temperature ($^{\circ}\text{C}$) | ≈ 200 | 20 |

Oil was fed into the throat of the venturi mist generator using a motorised syringe pump. The venturi reproduced conditions at the peak flow through the top ring a of a gasoline engine at 2500 rpm, 75% load and 50% throttle, as reported and derived from the model of Gamble et al. [28], Table 1. Dimensions are shown in Fig. 3. The lubricant inlet was raised approximately 1 mm above the venturi throat surface, so that the lubricant flowed over a distinct edge,

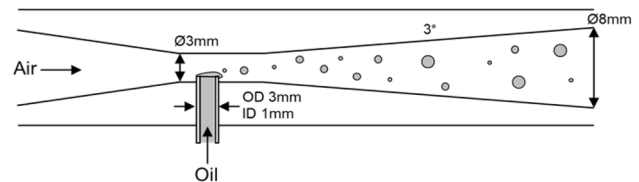


Fig. 3 Dimensions of Venturi mist generator

as in the piston ring gap. This feature was accounted for in the flow calculations. The expansion ratio of the venturi is the ratio of the outlet duct area to the throat area. The venturi was supplied with air from a laboratory compressed air supply via a coalescing filter with a $0.01 \mu\text{m}$ element and a pressure regulator. At an inlet air pressure of 0.15 MPa, the venturi was choked and the flow parameters are as listed in Table 1. Conditions correspond well to those in the engine in all but pressure and temperature. The effect of pressure was considered secondary as this mist formation mechanism is controlled by shear between the gas and lubricant flow, where similarity in velocity and flow rate is of greater importance. The lower temperature in the lab test may have influenced droplet formation and droplet size distribution, as viscometric, viscoelastic and extensional properties vary with temperature [41, 42]. Further work to measure droplet distributions extracted from the crankcase of a fired engine was performed: The effects of temperature on droplet

formation will be best clarified in future publications by comparing between the lab and engine environments.

The mist flow was directed, via an 8 mm pipe, through a laser diffraction particle sizer, that measured droplets with diameters between 0.1 and 1000 μm that passed through the 10 mm diameter beam. Data were collected continuously, recorded every second and averaged for the duration of the test. The distribution was presented as the proportion of the Total Flow Volume at each droplet diameter, the Volume Frequency: This was most relevant to bulk flow mechanisms, rather than number of droplets or proportion of the total surface area. Figure 4 shows a typical droplet size distribution. In this and almost all cases observed the distributions were tri-modal, i.e. three characteristic droplet diameter ranges. The largest had diameters of 135–1000 μm , typical of what is termed spray, where droplet inertia is high and they quickly deposit from the flow. These were not thought to form readily in the piston assembly, as they are of similar size to the ring gap. Droplets with diameters of 18–135 μm were present in almost every test. These droplets were typical of mist flows, where inertia is overcome by aerodynamic forces and droplets stay entrained in the gas flow, but are rapidly deposited from a flow as its velocity reduces. The smallest droplets, with diameters of 0.1–18 μm were typical of aerosol flows, where inertia is extremely low, entrainment in the gas flow is dominated by Brownian motion and, therefore, aerosol droplets are present even in stationary flows. Aerosol flows weren't present in many tests. The mist and aerosol droplets were thought to be representative of those found in the engine [43]. Aerosol and mist ranges were termed the minor and major misting region, respectively, in this study. Characteristic Droplet Diameters were defined

by the droplet diameter at the peak of each distribution bell curve.

The tendency to form droplets was measured by weighing the bulk liquid lubricant flowing into and out of the system. The lubricant entering the mist generator was calculated by weighing the syringe and feed line before and after each test and subtracting to find the difference. The oil that dripped from the outlet pipe was collected in a beaker and, again, weighed before and after the test. As this oil was not entrained in the gas flow, it was assumed to contain lubricant that has not formed droplets and/or droplets deposited on the pipe walls, i.e. this was unmisted oil. As it was not possible to collect all the droplets entrained in the gas flow, the weight of oil leaving the system as droplets was calculated by subtracting the unmisted oil from the total input:

$$M_{\text{droplets}} = M_{\text{in}} - M_{\text{unmisted out}}$$

where M_{droplets} is the total oil leaving the system as droplets, M_{in} is the total oil entering the system and $M_{\text{unmisted out}}$ is the total oil leaving the system unmisted. The tendency of a lubricant to form droplets was defined as total quantity of oil leaving the mist generator as droplets as a percentage of the total entering the system:

$$\% \text{ Droplets} = 100 \times \frac{M_{\text{droplets}}}{M_{\text{in}}}$$

In order that the measurements of the output values were more accurate, the outlet pipe from the mist generator was lined with PTFE so that oil would not wet the surface and be retained in the system, but would flow out under shear from the gas flow.

Fig. 4 Droplet size distribution for PAO 8 at 3 ml/min

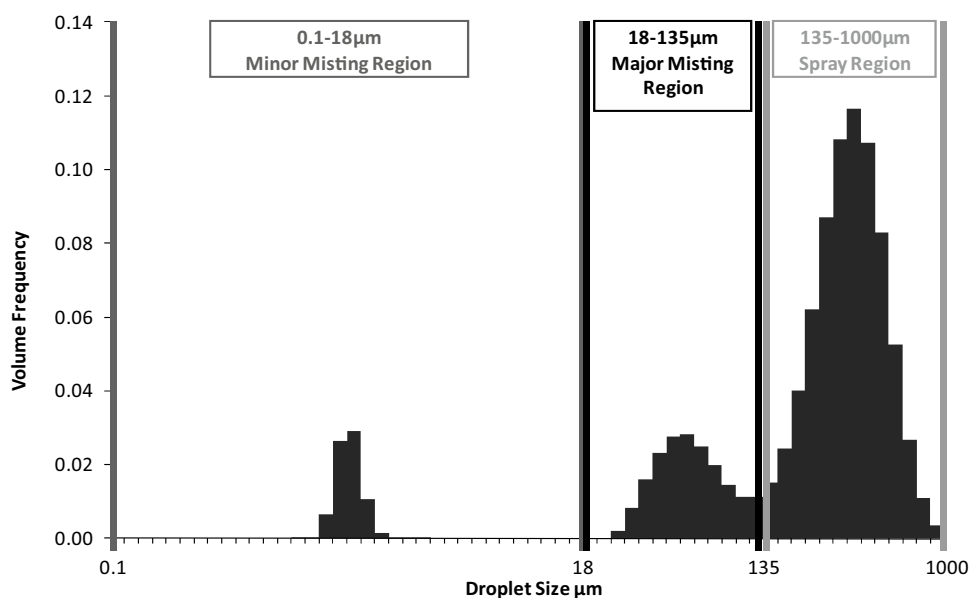


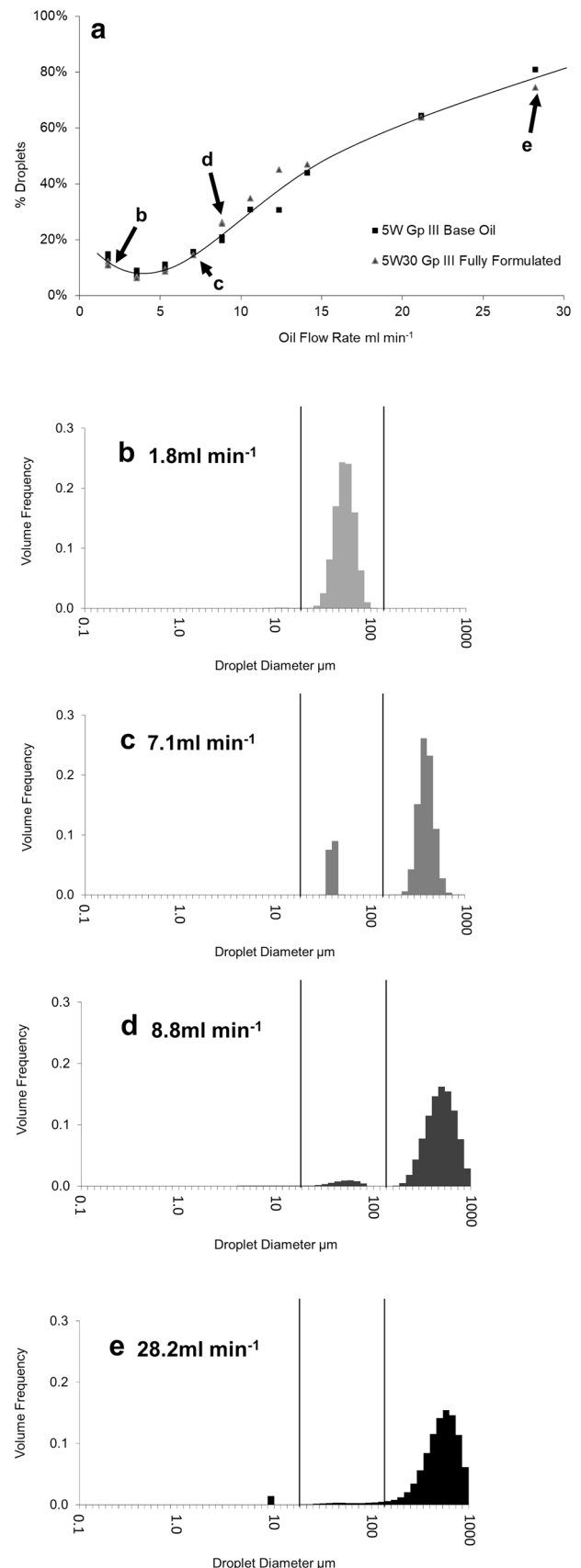
Fig. 5 Variation in droplets produced with oil inlet flow rate: **a** variation in misting tendency with oil inlet flow rate; droplet size distributions for fully formulated lubricant at; **b** 1.8 ml min⁻¹, **c** 7.1 ml min⁻¹, **d** 14.1 ml min⁻¹, **e** 28.2 ml min⁻¹

2.2 Procedure

The syringe charged with oil, the oil feed tube and the unmisted oil collection beaker, Fig. 2, were weighed. The syringe was compressed until the oil feed tube was full of oil. The particle sizer self-calibrated and data recording commenced. The air supply was switched on, set to 0.15 MPa and left for 10 s to allow the flow through the system to become steady. The syringe pump started and the inlet feed attached. The test duration was two minutes, starting when the oil entered the venturi (indicated by an audible change in gas flow). The test was ended by stopping the particle sizer and the syringe pump, clamping and disconnecting the oil feed pipe to prevent further oil flow. The air supply was kept running for a further 5 min to ensure that all oil was removed from the system. The mass change of the syringe, the oil feed tube, unmisted oil collection beaker, and the drip tray before and after the test provided M_{in} and $M_{unmisted\ out}$, and by subtraction $M_{droplets}$. Data from the particle sizer were recorded and averaged for the two-minute test period.

As the flow rate of air in the venturi was fixed, the misting process was controlled by the flow rate of oil. Figure 5 shows the misting tendency of an API Group III SAE 5W base oil and an API Group III 5W30 fully formulated lubricant at a range of oil inlet flow rates and the droplet size distributions at selected positions on the curve. As the inlet flow rate increased, the misting tendency initially decreased and then increased greatly above approximately 5 ml/min until almost all the oil formed droplets. At lower flow rates, the majority of droplets were in the major and minor misting regions. Above 9 ml/min, the droplets were almost entirely spray-sized droplets. It was hypothesised that a greater oil flow rate caused a greater accumulation of oil at the oil feed. Above a certain oil flow rate, approximately 9 ml/min in these cases, the droplet formation mechanism changed from ‘rolling’ to ‘undercutting’, as described by Hewitt et al. [44] and Fig. 6. The rolling mechanism was thought to be representative of the droplet formation at piston ring gaps and component edges. The undercutting mechanism was thought to be more representative of blow-through, e.g. at the cylinder-liner interface or in the oil control ring. Repeatability was low at low flow rates, below approximately 2.5 ml/min.

As both rolling and undercutting were representative of droplet formation mechanisms in the engine, the range of oil flow rates used in these tests was generally 3–9 ml/min, allowing observation of both mechanisms and the transition between them. For a small number of lubricants, the transition from rolling to undercutting occurred outside of this



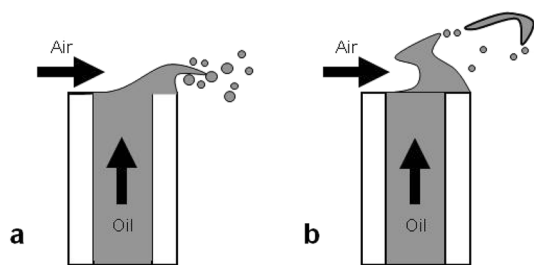


Fig. 6 Droplet formation mechanisms: **a** rolling, **b** undercutting, after [44]

range. Where feasible, the range was extended to accommodate this.

The undercutting mechanism was evaluated by considering several key parameters at a condition in the region of approximately linear increase in droplet formation tendency with oil inlet flow rate (i.e. significantly away from the transition so that the gradient of the curve was close to linear). An oil inlet flow of 9 ml/min met this condition for almost all lubricants. These parameters were %droplets, the gradient of the curve at this point and the linearly projected abscissa intercept of the curve from this point, Fig. 7.

The region of linear increase in droplet formation tendency was thought to be a superposition of the rolling droplet formation, which had low %droplets, and the undercutting droplet formation, which had higher %droplets. As the oil inlet flow rate increased, the quantity of lubricant at the throat of the venturi subject to the undercutting mechanism increased and the overall %droplets increased. Counterintuitively, a greater resistance to droplet formation by the undercutting mechanism produced a higher %droplets value, i.e. the resistance to droplet formation caused a greater quantity of the lubricant being exposed to the undercutting mechanism and a steeper curve. The complexity of

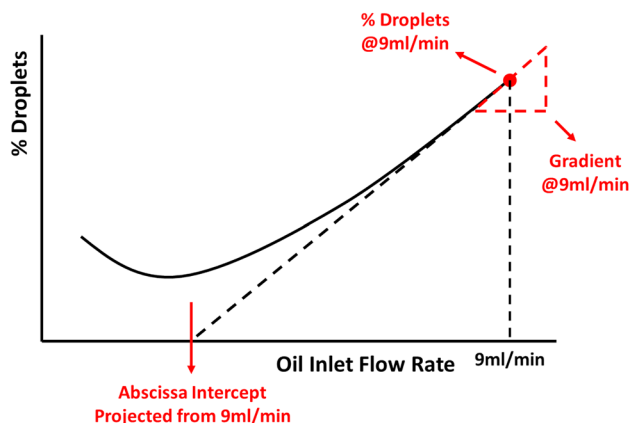


Fig. 7 Schematic of the comparative parameters used to describe behaviour in undercutting droplet formation, or blow-through

droplet formation is exemplified by this greater ‘resistance to shear and pressure-driven droplet formation’ causing more droplets to be produced, as lubricant accumulates and blows through rather than flowing.

2.3 Repeatability

Several repeated tests were conducted using different lubricants at various conditions. Parameters used to define the statistical significance of results and interpretations are in Table 2.

3 Stage 1 Investigation: The Influence of the Components of a Commercial Lubricant

The initial aim of this study was to determine the key characteristics of a commercial automotive lubricant that have the greatest effect on the tendency to form mist. Three aspects were considered:

1. Molecular weight and viscosity of the base oil
2. Molecular weight distribution of the base oil and comparing mineral oils to synthetics.
3. Additives used in a typical commercial lubricant

Test lubricants and their relevant properties are in Table 3. Molecular weight and viscosity of base oils were varied using four API Group IV polyalphaolefin (PAO) fluids of known molecular weight, and the same manufacturing process and feedstock: PAO 2, PAO 4, PAO 6 and PAO 8 in Table 3.

Molecular weight distribution of base oil was varied using SAE 5W grade base oils from Groups I-IV of the API base oil classification. Molecular weight distribution

Table 2 95% confidence intervals denoting the statistical significance of measured parameters

| Parameter | 95% confidence interval | | | |
|----------------------------|---|-------|-------|------|
| | Lubricant inlet flow rate (ml min ⁻¹) | | | |
| | 3 | 5 | 7 | 9 |
| %Droplets (%) | ±0.8 | ±1.3 | ±1.8 | ±1.0 |
| Volume fraction (%) | | | | |
| < 18 µm | ±3.3 | ±1.4 | ±1.0 | ±0.5 |
| 18–135 µm | ±11.7 | ±8.2 | ±3.4 | ±2.6 |
| > 135 µm | ±11.0 | ±8.0 | ±2.8 | ±2.8 |
| Mean droplet diameter (µm) | | | | |
| < 18 µm | ±1.4 | ±7.6 | ±7.0 | ±2.4 |
| 18–135 µm | ±9.1 | ±20.9 | ±15.7 | ±8.2 |
| > 135 µm | ±63 | ±101 | ±76 | ±18 |

Table 3 Description and key properties of lubricants tested

| Base Oil | | | Dynamic Viscosity @20°C, Pa.s | Kinematic Viscosity @100°C cSt | Additive | | Reference |
|-----------|-----------|---------------|-------------------------------|--------------------------------|--------------------|--------------------------------|-----------|
| API Group | SAE Grade | Ave. Mol. Wt. | | | Type | Chemistry | |
| IV | - | 285 | 7.97 | 1.9 | - | - | PAO 2 |
| IV | - | 436 | 32.16 | 4.0 | - | - | PAO 4 |
| IV | - | 530 | 62.02 | 6.1 | - | - | PAO 6 |
| IV | - | 600 | 97.99 | 7.8 | - | - | PAO 8 |
| I | 5W | - | 72.10 | 5.6 | - | - | Gp I |
| II | 5W | - | 65.89 | 5.4 | - | - | Gp II |
| III | 5W | - | 97.93 | 7.5 | - | - | Gp III |
| IV | 5W | 620 | 80.94 | 7.0 | - | - | Gp IV |
| III | 5W | - | 97.93 | 7.5 | - | - | Gp III |
| III | 5W30 | - | 130.15 | 9.3 | Viscosity Modifier | Poly(isoprene-co-styrene) Star | VM |
| III | 5W | - | 94.91 | 7.2 | Detergent 1 | Not Disclosed | Det 1 |
| III | 5W | - | 94.42 | 7.1 | Detergent 2 | Not Disclosed | Det 2 |
| III | 5W | - | 116.88 | 8.4 | Dispersant | Not Disclosed | Disp |
| III | 5W | - | 91.50 | 7.1 | Anti-foam | Silicone | AF |
| III | 5W30 | - | 115.36 | 9.6 | Fully Formulated | | FF |

around the average value decreases with increasing API Group: The increased refining of Groups 1 to 3 narrows the distribution and Group IV is a synthetic PAO with extremely narrow molecular weight distribution. There are differences in molecular structure between typical Group I-III oils and PAOs. PAOs are highly branched molecules, which can lead to differences in rheology, e.g. the pressure-viscosity relationship [20, 49]. There can be differences in saturation and branching between Groups I-III, but were not considered significant in this investigation. These oils had similar kinematic viscosity at 100 °C and comparable dynamic viscosity at 20 °C. These are Gp I, Gp II, Gp III and Gp IV in Table 3.

Additives were hypothesised to affect misting tendency by introducing changes in surface tension and/or viscoelastic properties. Therefore, surfactants (two detergent chemistries, dispersant, and silicone anti-foam) and polymeric viscosity modifiers were considered. These were added to the Group III SAE 5W base oil described previously at concentrations used in a commercial lubricant. For commercial reasons, concentrations and specific chemistries are not disclosed here. The fully formulated lubricant from which these formulations were derived, and the base oil used in this were included as reference values. These are Gp III, VM, Det 1, Det 2, Disp, AF and FF in Table 3.

4 Stage 1 Results and Discussion

4.1 Base Oil Molecular Weight and Viscosity

Figure 8 shows the misting tendency of PAOs of varying molecular weight and viscosity at a range of oil flow rates. At low flow rates, base oils with lower molecular weight and viscosity produced droplets more readily. As molecular weight and viscosity decreased, transition from a rolling to an undercutting mechanism occurred at a higher flow rate. This can be attributed to the lower resistance to shear exhibited by lower viscosity oils: Oil was more quickly removed from the venturi under shear and did not accumulate as much as a higher viscosity oil under the same conditions.

Figure 9 shows the variation in misting tendency of oil with average molecular weight. These were tests with an inlet oil flow rate of 3 ml/min, where the greatest proportion of mist-sized droplets was formed. Misting tendency varied inversely and linearly with molecular weight.

Figure 10 shows that the dynamic viscosity at 20 °C for these oils varied with molecular weight to the power of 3.35. Thus, misting tendency variation with dynamic viscosity at 20 °C can be described using a third order polynomial, Fig. 11, as could be expected from a combination of Fig. 9

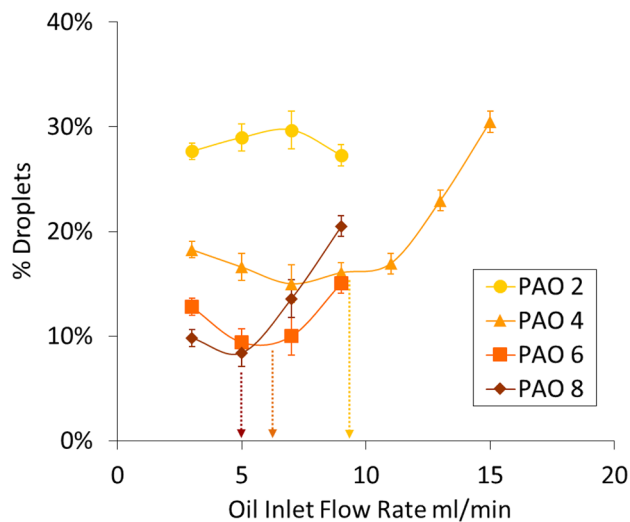


Fig. 8 Variation in misting tendency for PAOs of different average molecular weight

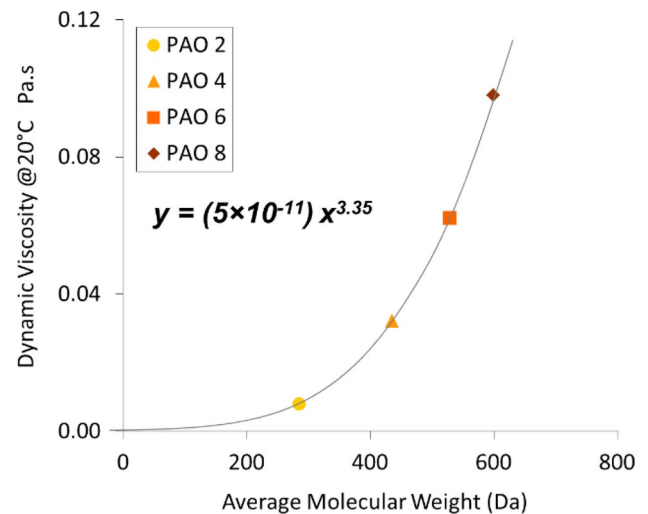


Fig. 10 Variation in dynamic viscosity at 20 °C for PAOs of varying average molecular weight

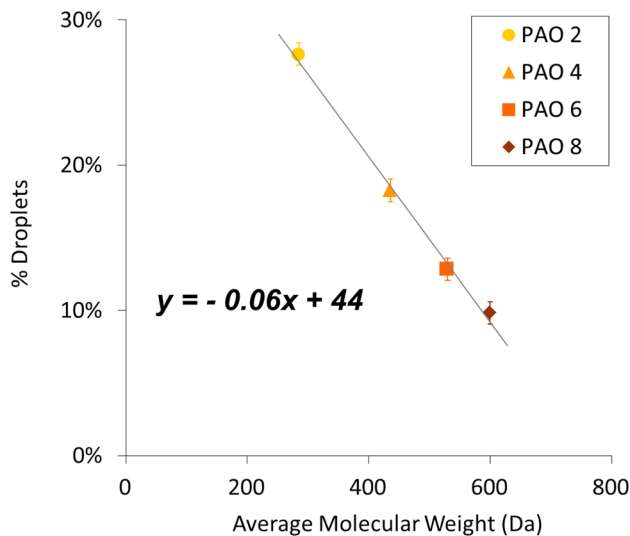


Fig. 9 Variation in misting tendency of PAOs with varying average molecular weight at 3 ml min⁻¹ oil inlet flow rate

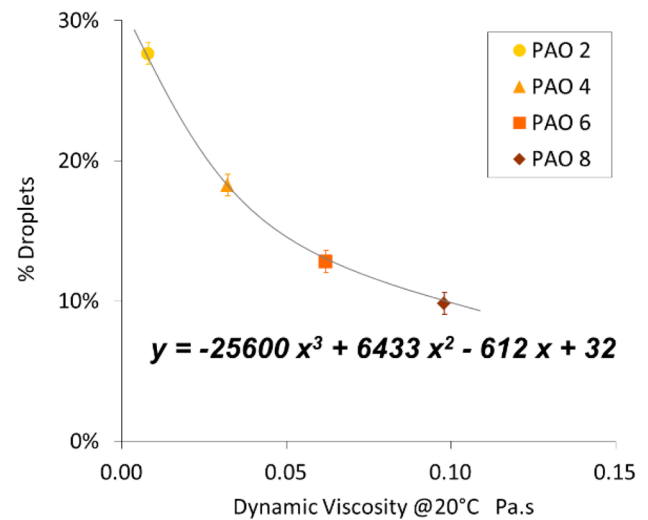


Fig. 11 Variation in misting tendency of PAOs with dynamic viscosity at 20 °C at 3 ml min⁻¹ oil inlet flow rate

and Fig. 10: Greatly increasing misting tendency with a decrease in dynamic viscosity.

Figure 12a–d shows the droplet size distributions for the tests described in Fig. 9 and Fig. 11. As the proportion is volumetric, the apparently substantial proportion of spray in these distributions was contained in relatively few droplets. There was a large quantity of mist-sized droplets in each distribution, especially in the major mist region. PAO 2 and PAO 6 had comparable characteristic diameters, approximately 34 μm . PAO 8 had a larger characteristic diameter, approximately 63 μm , consistent with previous findings that higher viscosity oils produce larger droplets [45, 46]. The

distribution for PAO 4 was different but the reason for this was not clear.

4.2 Base Oil Molecular Weight Distribution

Figure 13 shows the variation in misting tendency of oils with similar viscosity but of different API Groups, again at an oil inlet flow rate of 3 ml/min. Fully formulated reference oil was included for comparison. There was no significant difference in the misting tendencies between the refined oils (I–III). Group IV oil, PAO, showed significantly greater misting tendency. This may arise from differences in molecular structure between refined hydrocarbons (slightly branched

Fig. 12 Droplet size distributions for PAOs of varying average molecular weight at an oil inlet flow rate of 3 ml min^{-1} : **a** PAO 2, **b** PAO 4, **c** PAO 6, **d** PAO 8

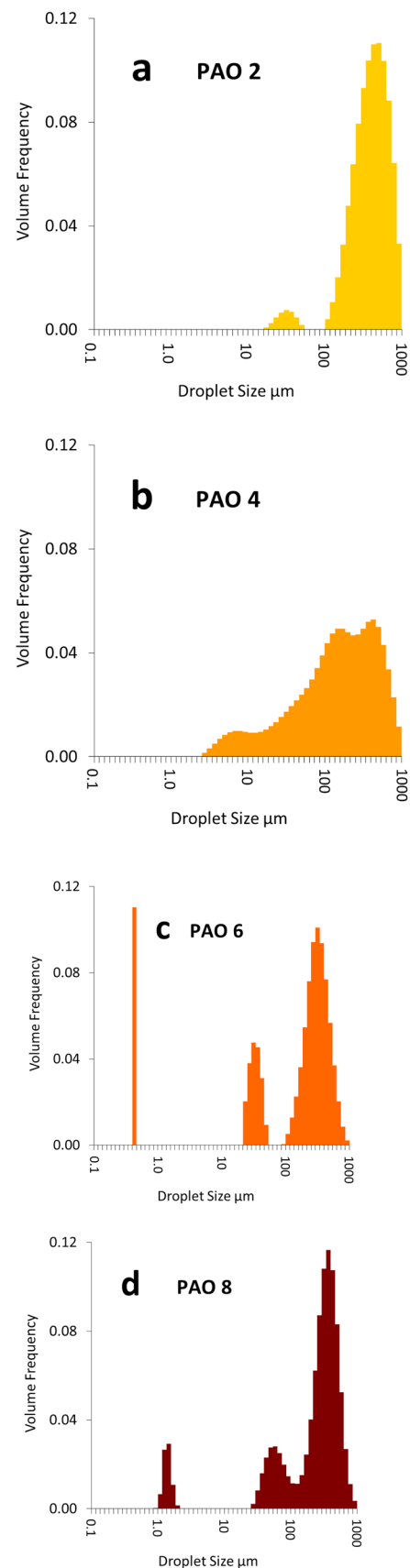
linear chains) and PAO, which is mainly trimer and tetramer of decane with a star-type structure.

4.3 Common Commercial Additives

Figure 14 shows the misting tendency of Group III SAE 5W lubricants containing single commercial additives at an oil inlet flow rate of 3 ml/min . The commercial fully formulated lubricant, FF, and the base oil reference, Gp III, were included. Fully formulated lubricant had a much lower tendency to form droplets than its base oil under the same conditions. The blend containing viscosity modifier, VM, behaved comparably to the fully formulated lubricant, indicating that VM has a dominant role in reducing misting tendency. Detergent 2, Det 2, and silicone antifoam, AF, significantly increased misting tendency. Detergent 1, Det 1, or dispersant, Disp, did not significantly affect the misting tendency of the base oil. Some additives altered the viscosity, Table 3, but viscosity didn't correlate significantly with misting tendency in Fig. 14.

Figure 15 shows the droplet size distributions for the tests in Fig. 14. Distributions for the fully formulated lubricant and the viscosity modifier blend were narrow with no clear pattern. The relatively small quantities of droplets, due to the influence of the viscosity modifier, caused these tests to have less statistical repeatability than for lubricants with higher misting tendency. Droplets in the major mist region for the reference base oil, the blends containing viscosity modifiers or detergent have similar characteristic diameter, approximately $46 \mu\text{m}$. The distribution for oil containing antifoam was tetramodal with two characteristic diameters in the major mist region. The distribution for oil containing dispersant had characteristic sizes outside the established regions. Significant quantities of minor mist-sized droplets were observed when surface-active additives were present, i.e. detergents, dispersant and antifoam. These additives probably affected the liquid/air interfacial properties: This could be investigated using, e.g. the Weber Number [47], the ratio between inertia and surface tension forces, but was beyond the scope of this study.

Including a polymeric viscosity modifier had the greatest effect on reducing the misting tendency of lubricants. The viscoelastic properties of such polymer-containing fluids alter the extensional behaviour. As discussed by Dasch et al. [38], Marano et al. [45] and Smolinski et al. [46], higher extensional viscosity induced by the presence of polymers reduces the tendency of a fluid to break into droplets under shear and extension. These effects were more significant than changes in surface properties induced by the



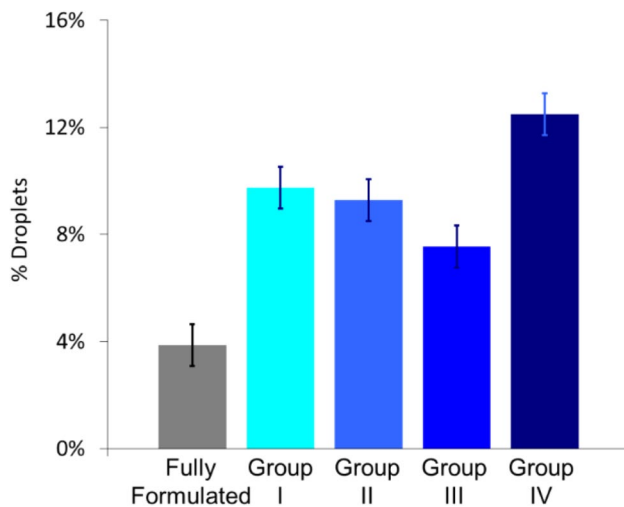


Fig. 13 Variation in misting tendency for oils in different API groups with similar dynamic viscosities at 20 °C at an oil inlet flow rate of 3 ml min⁻¹

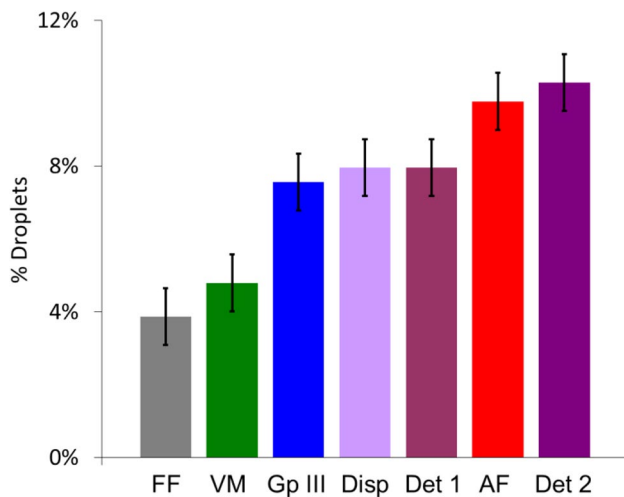


Fig. 14 Variation in misting tendency for Group III SAE 5W oil containing various additives with an oil inlet flow rate of 3 ml min⁻¹

presence of surface-active additives; detergents, dispersant and antifoam. This broadly correlated with the observations of Ohmori et al. [48], where polymer additives significantly increased extensional breakup time, but that surfactant additives had little effect.

5 Stage 2: Detailed Consideration of Viscosity Modifiers

Because of dominant influence of viscosity modifiers in Stage 1, seven types were compared, varying in molecular structure, molecular weight, chain length, etc. Four linear polymers and three star polymers were used. Three of the

linear were olefin copolymers (OCPs), copolymers of ethylene and propylene, varying in molecular weight over an order of magnitude. The fourth was a poly-styrene-co-isoprene with a longer chain length than the largest of the OCP polymers. Two of the star polymers were fixed star structures, one isoprene and one isoprene-co-styrene. The third was a micellar styrene-co-isoprene, where arms formed a star structure through association of their end groups. These are shown in Table 4 with the following properties:

- Number average molecular weight—Measured using gel permeation chromatography (GPC).
- Ratio of monomers—Estimated from manufacturer's descriptions.
- Average monomer weight—Calculated from chemical structure and ratio of monomers.
- Chain length per monomer—Calculated from chemical structure and ratio of monomers.
- Entanglement molecular weight—Given for linear solid polymers by Ferry [49].
- Number of arms—Estimated from manufacturer's patent literature.
- Arm molecular weight—Calculated from number average molecular weight and number of arms.
- Chain length—Calculated from number average molecular weight, average molecular weight and chain length per monomer.

Three blends per polymer were formulated, Fig. 16. Two API Group III base oils were used: One with a KV100 (nominal kinematic viscosity at 100 °C) = 4cSt and the other with KV100 = 8cSt. From these, two blends with KV100 = 12cSt were produced, one from each base oil. A third blend KV100 = 8cSt was produced from the 4cSt base oil. Different polymers required different concentrations to achieve the same viscosity. Viscosity modifiers are typically included in engine oils at concentrations of 7%wt to 10%wt [52]. However, in most formulations, these are concentrates of polymer diluted in a base oil. Concentrates contain typically 6%wt to 15%wt polymer [52], i.e. VM polymer concentration is approximately 0.4%wt to 1.5%wt [52]. Where possible, polymer concentrations were in this range, Table 5. Viscosity index (VI) was calculated using ASTM D2270 [53].

The entanglement properties, molecular size and viscoelasticity of the blends were characterised. Entanglement properties were calculated in two ways: Firstly, from theory developed by Ferry [49] and Graessley [50]. The entanglement molecular weight, Fig. 17, for a pure, solid and linear polymer was virtually 'diluted' until the concentration of polymer was equivalent to that in the real blend. The new entanglement molecular weight was calculated using the following equation:

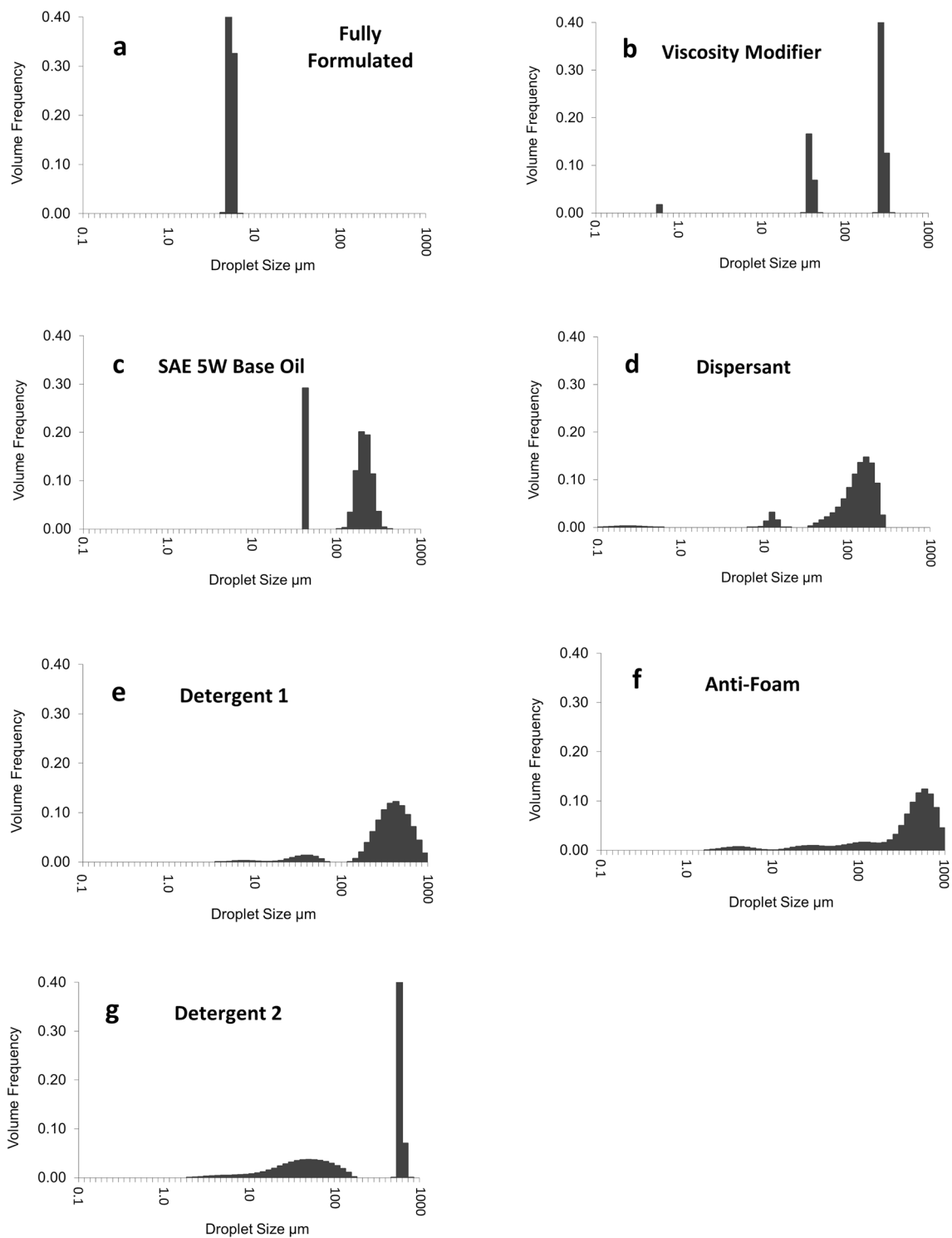
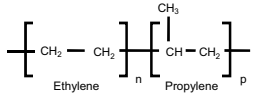
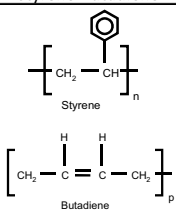
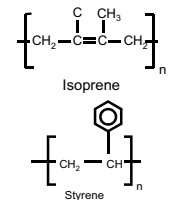
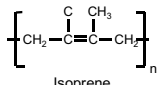
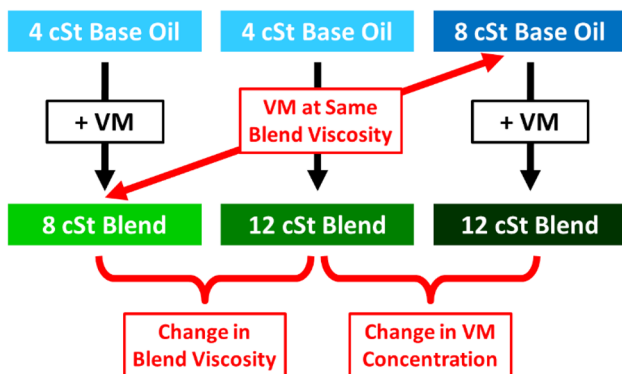


Fig. 15 Droplet size distributions for SAE 5W API Group III base oil with additives, at an oil inlet flow rate of 3 ml min^{-1} : **a** fully formulated reference, **b** viscosity modifier, **c** SAE 5W API Group III base oil reference, **d** Dispersant, **e** detergent 1, **f** anti-foam, **g** Detergent 2

Table 4 Polymers tested and their key properties, with reference to Ferry [49], Graessley [50] and Rhodes [51]

| | Linear | | | Star | | | |
|--|---|--------------------|--------------------|--|---|---|-----------------|
| | Olefin Copolymer | | | Styrene-Butadiene | Isoprene-co-Styrene | | Isoprene |
| |  | | |  |  |  | |
| Reference | 1 | 2 | 3 | 4 | 5 | 6 | 7 |
| Ratio of Monomers (estimated from manufacturers data) | E = 50% P = 50% | E = 20% P = 80% | E = 50% P = 50% | S = 50% B = 50% | I = 80% S = 20% | I = 50% S = 50% | I=100% |
| Number Average Molecular Weight M_n (Da) (from GPC) | 51945 | 42359 | 2997 | 75412 | 146499 | 65039 | 80003 |
| Average Monomer Molecular Weight M_o (Da) (from Graessley [44]) | 34.3 | 39.2 | 34.3 | 65.5 | 75 | 86 | 68 |
| Chain Molecules per Monomer j (from Graessley [44]) | 2 | 2 | 2 | 4 | 3.6 | 3 | 4 |
| Entanglement Molecular Weight $M_{e,max}$ (Da) (From Ferry [43]) | 1660 | 1250 | 1660 | 3000 | 8572 | 12145 | 4706 |
| Number of Arms (Estimated from Rhodes [45]) | - | - | - | - | 10 | 10 | 10 |
| Arm Molecular Weight M_o (Da) (Calculated) | - | - | - | - | 14650 | 6503 | 8000 |
| Chain Length (Calculated) | 3028 | 2161 | 175 | 4605 | 7031 (1 arm) | 2289 (1 arm) | 4706 (1 arm) |

**Fig. 16** Scheme of test lubricant blends

$$M_{EBlend} = M_E c^{-1.3}$$

where M_E is the entanglement molecular weight and c is the volumetric concentration of the polymer.

From this, the entanglement density was calculated:

$$E_{Blend} = E c^{1.3} = \frac{M c^{1.3}}{M_E}$$

where E is the entanglement density and M is the number average molecular weight of the polymer. When the entanglement density exceeded 0.1, the blend was considered semi-dilute [50], where there is significant

intermolecular-molecule interaction but not large-scale entanglement. However, this approach doesn't account for the variation in intermolecular interaction caused by temperature and shear. Data for the solid entanglement molecular weights are reported by Ferry [49]. Entanglement of star polymers correlates better with the molecular weight of individual arms rather than the whole molecule: The hindered structure affects intermolecular interaction. Thus, for star polymers, the equation is:

$$E_{ABlend} = E_A c^{1.3} = \frac{M_A c^{1.3}}{M_E}$$

where M_A is the average molecular weight of an individual arm, estimated from Rhodes [51], and E_A is the entanglement density of the polymer considered as individual arms.

Secondly, the theory of Schulz et al. [54] and Graessley [50] was used, where Gel Permeation Chromatography (GPC) was used to measure the radius of gyration (R_G) of each polymer in a good solvent. R_G is the radius of the generalised spherical volume the polymer molecule occupies and influences. From R_G the self-concentration ($c_{molecule}$) was calculated, i.e. the volumetric concentration of the polymer in the volume of base oil it occupied and influenced:

$$c_{molecule} = \frac{3M}{4\pi N_A R_G^3}$$

where N_A is Avogadro's Number.

Table 5 Characterisation of polymers and blends

| Polymer | Type | Polymer Concentration | Kinematic Viscosity @100°C | Dynamic Viscosity @20°C | VI | M_e | $M_{e \text{ Blend}}$ | E_{Blend} | R_G | HDV | C_{molecule} | l_p |
|----------------|-----------------------------------|-----------------------|----------------------------|-------------------------|-----|--------|-----------------------|--------------------|-------|------|-----------------------|-------|
| | | (%wt) | (cSt) | (mPa.s) | | (Da) | (Da) | (nm) | | | | |
| 1 | Olefin Copolymer | 1.00% | 8.4 | 77.0 | 187 | 1,660 | 606,852 | 0.086 | 8.2 | 2.3 | 4.8 | 1.65 |
| | | 1.90% | 13.0 | 129.0 | 193 | | 263,664 | 0.197 | | | | |
| | | 0.70% | 12.1 | 161.3 | 157 | | 947,926 | 0.055 | | | | |
| 2 | Olefin Copolymer | 1.16% | 8.4 | 85.7 | 177 | 1,250 | 367,534 | 0.115 | 8.1 | 2.2 | 4.1 | 1.41 |
| | | 1.90% | 12.7 | 141.4 | 189 | | 193,681 | 0.219 | | | | |
| | | 0.80% | 11.9 | 183.3 | 147 | | 585,245 | 0.072 | | | | |
| 3 | Olefin Copolymer | 6.20% | 7.7 | 81.9 | 164 | 1,660 | 56,883 | 0.053 | 1.9 | 0.03 | 22.3 | 1.77 |
| | | 10.90% | 12.2 | 148.4 | 186 | | 27,431 | 0.109 | | | | |
| | | 4.80% | 12.4 | 194.2 | 148 | | 77,930 | 0.038 | | | | |
| 4 | Styrene-Butadiene | 0.83% | 8.4 | 86.6 | 175 | 3,000 | 1,763,473 | 0.043 | 9.9 | 4.1 | 3.3 | 1.37 |
| | | 1.25% | 11.8 | 129.0 | 186 | | 1,034,977 | 0.073 | | | | |
| | | 0.62% | 12.9 | 194.5 | 155 | | 2,532,847 | 0.030 | | | | |
| 5 | Styrene-co-Isoprene | 0.70% | 7.7 | 70.8 | 180 | 8,572 | 1,293,534 | 0.011 | 11.2 | 5.9 | 15.2 | 7.13 |
| | | 1.30% | 12.1 | 127.1 | 194 | | 587,630 | 0.025 | | | | |
| | | 0.52% | 12.3 | 187.2 | 150 | | 1,862,237 | 0.008 | | | | |
| 6 | Styrene-co-Isoprene Micellar-type | 1.46% | 8.5 | 78.4 | 196 | 12,145 | 718,941 | 0.009 | 10.8 | 5.3 | 7.5 | 3.40 |
| | | 1.78% | 11.9 | 115.4 | 206 | | 560,275 | 0.012 | | | | |
| | | 0.90% | 11.9 | 167.4 | 159 | | 1,306,393 | 0.005 | | | | |
| 7 | Isoprene | 1.00% | 8.2 | 80.8 | 181 | 6,190 | 592,157 | 0.014 | 10.4 | 4.7 | 10.4 | 4.52 |
| | | 1.78% | 13.0 | 139.0 | 195 | | 285,558 | 0.028 | | | | |
| | | 0.80% | 13.3 | 200.0 | 156 | | 773,930 | 0.010 | | | | |
| 4 cSt Base Oil | | - | 4.4 | 43.2 | - | - | - | - | - | - | - | - |
| 8 cSt Base Oil | | - | 8.1 | 107.4 | - | - | - | - | - | - | - | - |

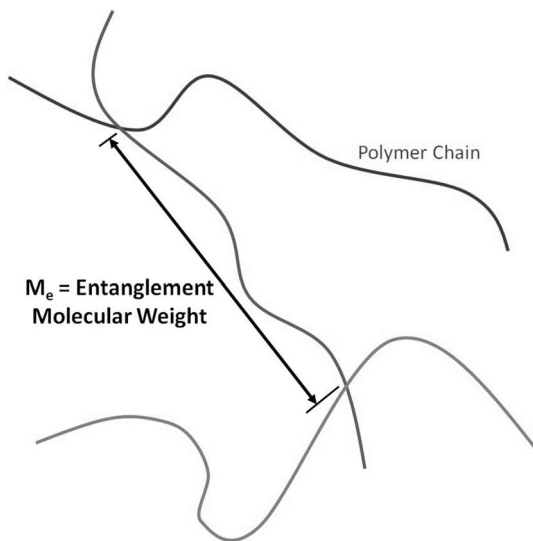


Fig. 17 Schematic of polymer entanglement molecular weight M_e

When the volumetric concentration of polymer in the bulk blend approaches the self-concentration of the polymer, $c_{\text{molecule}} \approx c$, the occupied volumes of the individual molecules start to overlap, i.e. more interaction and entanglement: The blend is considered semi-dilute. c_{molecule} can also describe polymer molecule coiling, i.e. higher c_{molecule} means a greater degree of coiling relative to another polymer of comparable molecular structure under comparable conditions.

The linear viscoelasticity of each blend was characterised using an oscillating test sequence on a parallel plate rheometer. In linear viscoelasticity Hooke’s Law applies, where response to strain is linear and cycle-to-cycle variation under the same conditions does not occur. Using a constant frequency and steadily increasing the amplitude, the viscoelastic responses for all blends were linear up to at least 5% strain. Thus, in a subsequent test, the frequency of oscillating shear was increased for a constant maximum strain of 5%, increasing the shear rate until the elastic modulus became greater than the viscous modulus, i.e. where solid properties began to dominate. The shear stress at this point was recorded.

The hydrodynamic volume (HDV) of the polymer, the volume of fluid an average individual polymer molecule occupies and influences, was calculated from the following equation [50]:

$$HDV = \frac{4\pi R_G^3}{3}$$

The packing length was calculated using the following equation [50], indicating how well coiled or extended an average molecule was:

$$l_p = \frac{M}{\rho N_a R_G^2}$$

where ρ is the density of the polymer as a solid.

6 Stage 2 Results and Discussion

6.1 Characterisation of Polymers and Blends

Table 5 shows polymer and blends properties. Only a few blends had were semi-dilute (i.e. entanglement density > 0.1), generally high concentration linear polymer blends. Star polymers had entanglement densities around an order of magnitude lower than linear polymers, i.e. no significant intermolecular interaction. At engine temperatures, larger hydrodynamic volumes could cause semi-dilute interactions in more blends.

Polymers 1 and 2, high molecular weight linear OCPs, had similar hydrodynamic volumes, but Polymer 1 had higher self-concentration, indicating tighter coiling. Polymer 3, a low molecular weight OCP, had extremely small hydrodynamic volume and extremely high self-concentration relative to other OCPs. This indicated either extreme high coiling or that molecules were sufficiently short to not coil significantly. The latter was more likely, suggesting low potential for further extension of Polymer 3 molecules.

Polymer 4, a high molecular weight styrene-butadiene, produced the lowest entanglement densities of the linear polymers. The thickening effect was high, so concentrations were relatively low. The large hydrodynamic volume and low self-concentration indicated low coiling. The larger styrene side groups appeared to hinder coiling. Thus, the potential for extension of this molecule was lower than an OCP of similar chain length [55].

Polymers 5 to 7, star polymers, showed different behaviour. Hydrodynamic volumes were higher than the linear polymers. Due to the dense molecule core and the coiling of the arms, self-concentration was extremely high. However, as the arms are fixed in the core, or physically attracted (Polymer 6), bending and extension was hindered, hence the stronger correlation with arm molecular weight than total molecular weight [50].

6.2 Misting Behaviour

Figure 18 and Table 6 show misting tendency and droplet distribution characteristics for polymer blends at low inlet flow rate, 3 ml/min, ‘rolling’ or misting conditions. Table 7 and Table 8 show droplet formation parameters and droplet distribution characteristics for polymer blends at higher inlet flow rate, 9 ml/min, i.e. ‘undercutting’ or blow-through conditions.

Figure 19 shows droplet formation tendency and droplet size distribution at 3 ml min⁻¹ for Polymer 1, a high molecular weight OCP. Droplet formation tendency was

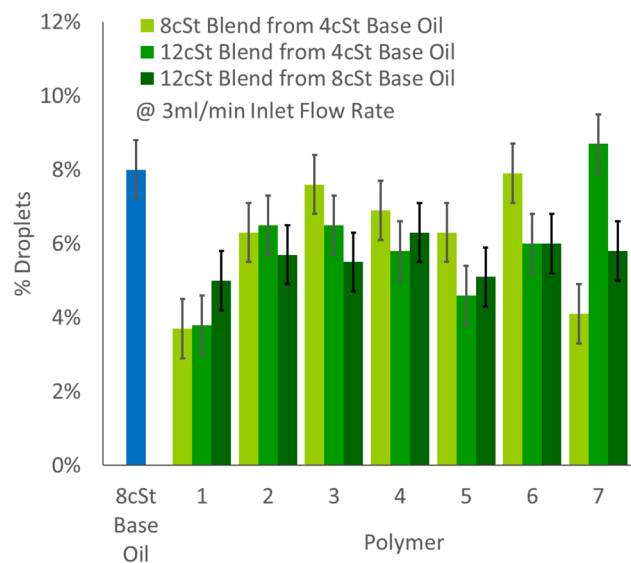


Fig. 18 %Droplets for all lubricants at an oil inlet flow rate of 3 ml/min

dramatically reduced under all conditions. Behaviour was independent of polymer concentration and viscosity. There was a relatively high proportion of mist-sized droplets, 27.8–60.7%, Table 6, and an increase in the characteristic droplet diameters in blends using higher viscosity base oil, 73 μm versus 40–54 μm .

Figure 20 shows results for Polymer 2, a high molecular weight OCP. Droplet formation tendency was reduced by 1.5–2.3% at 3 ml min⁻¹, Fig. 18. The proportion of mist and aerosol (6.0–12.5%) was greatly reduced versus 8cSt base oil (60.7%), Table 6. Transition to undercutting occurred at lower flow rate, Table 7. At high flow rates, droplet formation tendency increased with polymer concentration. Characteristic spray droplet diameters were greater under all conditions (540 μm) than 8cSt base oil (460 μm). Mist was suppressed in the 8cSt blend and aerosol was suppressed in the 12cSt blend from 8cSt base oil. Characteristic mist droplet diameter was greater at the highest polymer concentration, 63 μm versus 40 μm , Table 8.

Figure 21 shows results for Polymer 3, a low molecular weight OCP. Droplet formation tendency correlated with blend viscosity: The 8cSt blend and 8cSt base oil were insignificantly different, as also for 12cSt blends. There was relatively high proportion of mist and aerosol (39.7% for 8cSt blend versus 60.7% for 8cSt base oil) and the consistent presence of aerosol-sized droplets with diameters of $\sim 0.5 \mu\text{m}$, Table 6, Fig. 21. Some blends were semi-dilute but entanglement effects were not significant. Base oil dependency was seen, Table 7: Abscissa intercepts for 8cSt and 12cSt blends from 4cSt base oil were insignificantly different, but was greater for the 12cSt blend from 8cSt base oil.

Table 6 Characteristic droplet diameters and droplet size proportions for polymer blends at an inlet flow rate of 3 ml/min, ‘rolling’ conditions

| | 8cSt Base Oil | | | 8cSt (from 4cSt) | | | 12 cSt (from 4cSt) | | | 12cSt (from 8cSt) | | |
|---------|--|--------|--------|------------------|--------|--------|--------------------|--------|--------|-------------------|--------|--------|
| Polymer | Characteristic Droplet Sizes (µm) @3ml/min | | | | | | | | | | | |
| | Aero. | Mist | Spray | Aero. | Mist | Spray | Aero. | Mist | Spray | Aero. | Mist | Spray |
| 95% CI | ± 1.4 | ± 9.1 | ± 63 | ± 1.4 | ± 9.1 | ± 63 | ± 1.4 | ± 9.1 | ± 63 | ± 1.4 | ± 9.1 | ± 63 |
| 1 | 8.5 | 46 | 215 | 15 | 54 | 400 | 7.5 | 40 | 215 | 1 | 73 | 630 |
| 2 | | | | 0.5,10 | - | 540 | 8.5 | 63 | 630 | - | 40 | 400 |
| 3 | | | | 0.6 | 63 | 630 | 0.5 | 30 | 460 | 0.7 | 46 | 400 |
| 4 | | | | 0.3, 8.5 | - | 400 | - | 54 | 630 | 0.4, 10 | - | 540 |
| 5 | | | | 8.5 | 116 | - | - | - | 460 | - | - | 540 |
| 6 | | | | 1.2,13 | - | 540 | 1.2 | 54 | 630 | - | - | 460 |
| 7 | | | | 4.6 | 29 | 730 | 6.3 | 34 | 290 | 13 | - | 460 |
| | Droplet Size Volume Proportions (%) @3ml/min | | | | | | | | | | | |
| | Aero. | Mist | Spray | Aero. | Mist | Spray | Aero. | Mist | Spray | Aero. | Mist | Spray |
| 95% CI | ± 3.3 | ± 11.7 | ± 11.0 | ± 3.3 | ± 11.7 | ± 11.0 | ± 3.3 | ± 11.7 | ± 11.0 | ± 3.3 | ± 11.7 | ± 11.0 |
| 1 | 35.0 | 25.7 | 39.3 | 11.0 | 50.7 | 38.3 | 3.9 | 23.7 | 72.4 | 0.1 | 9.3 | 90.7 |
| 2 | | | | 6.0 | - | 94.0 | 5.8 | 6.7 | 87.5 | - | 9.6 | 90.4 |
| 3 | | | | 1.2 | 38.5 | 60.3 | 3.5 | 8.1 | 88.4 | 1.6 | 24.9 | 73.5 |
| 4 | | | | 16.3 | - | 83.7 | 9.4 | 49.6 | 40.9 | 7.3 | - | 92.7 |
| 5 | | | | 4.9 | 60.0 | 35.1 | - | - | 100 | - | - | 100 |
| 6 | | | | 1.8 | 0.0 | 98.2 | 0.1 | 5.1 | 94.8 | - | - | 100 |
| 7 | | | | 9.0 | 39.8 | 51.2 | 2.3 | 19.1 | 78.6 | 3.1 | 7.5 | 89.4 |

95% CI denotes the statistical confidence interval. Some distributions have two characteristic sizes in a range (separated by commas)

Figure 22 shows results for Polymer 4, a high molecular weight styrene-butadiene. Polymer-dominated behaviour was indicated by differences in droplet formation between 8cSt blend and 8cSt base oil. However, viscosity dependence was greater, indicated by similar droplet formation tendency for 12cSt blends despite different polymer concentration, Tables 6 and 8. There was some aerosol formation.

Figure 23 shows results for Polymer 5, a high molecular weight styrene-isoprene star. 12cSt blends produced similar sized droplets, larger than the 8cSt blend (460–540 µm vs. 116 µm), Table 6. The 8cSt blend produced a significant quantity of aerosol (4.9%). Misting tendency correlated with viscosity, also characteristic droplet diameters for spray. There was insignificant difference in misting tendency between the 12cSt blends, and between the 8cSt base oil and 8cSt blend, Fig. 18

Table 7 Comparative parameters for blow-through of lubricants

| | 8cSt Base Oil | 8cSt (from 4cSt) | 12 cSt (from 4cSt) | 12cSt (from 8cSt) |
|----------------|--|------------------|--------------------|-------------------|
| Polymer | % Droplets @9ml/min (% ±0.8) | | | |
| 1 | 18.9% | 8.2% | 2.9% | 2.5% |
| 2 | | 25.0% | 34.1% | 27.7% |
| 3 | | 19.2% | 23.7% | 26.6% |
| 4 | | 23.5% | 31.4% | 28.2% |
| 5 | | 18.2% | 29.8% | 26.1% |
| 6 | | 20.2% | 29.7% | 23.1% |
| 7 | | 20.1% | 24.6% | 29.0% |
| Polymer | Gradient @9ml/min (%/(ml/min) ±0.4) | | | |
| 1 | 4.0 | 2.0 | 1.1 | 0.2 |
| 2 | | 6.3 | 8.0 | 6.5 |
| 3 | | 3.9 | 5.3 | 7.5 |
| 4 | | 4.4 | 7.3 | 5.4 |
| 5 | | 3.2 | 6.6 | 5.6 |
| 6 | | 4.9 | 5.9 | 5.0 |
| 7 | | 4.3 | 5.0 | 6.8 |
| Polymer | Abscissa Intercept @9ml/min (ml/min ±0.3) | | | |
| 1 | 4.3 | 6.9 | 8.2 | -3.0 |
| 2 | | 3.0 | 2.7 | 2.8 |
| 3 | | 4.1 | 4.5 | 5.4 |
| 4 | | 3.7 | 2.7 | 1.8 |
| 5 | | 3.4 | 2.5 | 2.3 |
| 6 | | 4.9 | 1.9 | 2.3 |
| 7 | | 2.4 | 4.1 | 2.7 |

Figure 24 shows results for Polymer 6, a micellar-type styrene–isoprene star polymer. The star structure of this polymer dissociates under shear into individual arms of short chain linear polymers (molecular weight ~ 6500 Da, around 30% greater than Polymer 3, i.e. low). Misting tendency of the 8cSt blend was insignificantly different to 8cSt base oil, Fig. 18, and there was significant formation of aerosol (0.1–1.8%), Table 6. Because blend viscosity was calibrated to the star structure, dissociation will have changed the high shear viscosity: Droplet formation curves had similar profiles but varying abscissa intercepts, Table 7.

Figure 25 shows results for Polymer 7, a high molecular weight fixed isoprene star. Viscosity dependence was greater than viscoelastic effects. The 12cSt blends behaved comparably overall, producing higher proportions of spray than the 8cSt blend (78.6–89.4% vs. 51.2%), Tables 6 and 8. The 8cSt polymer blend generated lower aerosol proportion (9.0% vs. 35.0%) than 8cSt base oil, Table 6.

7 Comparison Between Viscosity Modifiers

7.1 Different High Molecular Weight Fixed Stars: Polymers 5 and 7

At low flow rate, misting conditions, the higher molecular weight star (Polymer 5) produced larger mist and aerosol droplets in 8cSt blends, Fig. 18. In 12cSt blends, the high molecular weight star suppressed mist and aerosol formation substantially: The lower molecular weight star reduced mist and aerosol proportion substantially versus 8cSt base oil.

Behaviour at high flow rates, spray conditions, was similar for both polymers except that, in Polymer 7, the 12cSt blend from an 4cSt base oil had lower misting tendency than the 12cSt blend from an 8cSt base oil—Inverse to Polymer 5, Table 7. Although the smaller molecules of Polymer 7 store less energy individually than Polymer 5 (lower self-concentration and arm molecular weight), higher concentration was required to achieve the blend viscosity, so perhaps the total quantity of potential extensional energy per unit finished blend was higher. This suggests that potential viscoelastic energy could be controlled somewhat independently of thickening effect.

7.2 Fixed and Micellar Star Polymers: Polymers 5 and 7, and Polymer 6

At low flow rates, 3 ml/min, misting conditions, the micellar star polymer (Polymer 6) produced less mist and aerosol in 8cSt blends than fixed star Polymers 5 and 7 (1.8% vs. 48.8% and 64.9%), Table 6. Dissociation means micellar star arms are, functionally, linear polymers, so energy dissipation may be greater than fixed star arms, which are constrained at one end and hindered.

At high flow rate, 9 ml/min, spraying conditions, the micellar star polymer produced more mist and aerosol-sized droplets than fixed stars (7.4% vs. 1.3% and 2.8%), Table 8. Projected abscissa intercepts for micellar stars varied due to micelle dissociation affecting viscosity, Table 7. Overall, differences in misting tendency under spray conditions correlated more strongly with viscosity. For all star polymers, fewer aerosol-sized droplets were formed in higher viscosity base oil (12cSt blend from 8cSt base oil).

7.3 Differences in High Molecular Weight OCPs: Polymers 1 and 2

Polymer 1 greatly suppressed droplet formation but Polymer 2 did not generate such dramatic reduction. Polymer 1 was more tightly coiled and had greater capacity for energy dissipation in extension. At low flow rate, 3 ml/min, misting

Table 8 Characteristic droplet diameters and droplet size proportions for polymer blends at an inlet flow rate of 9 ml/min, blow-through conditions

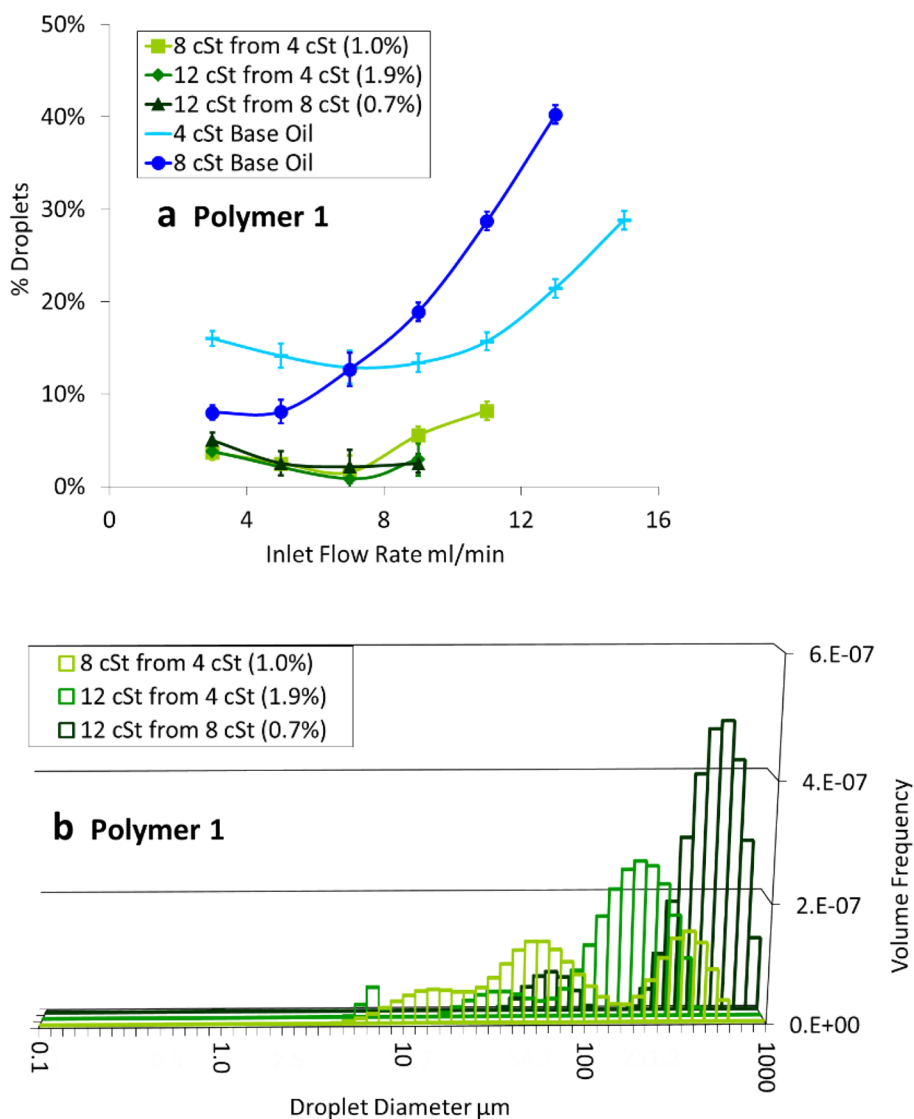
| | 8cSt Base Oil | | | 8cSt (from 4cSt) | | | 12 cSt (from 4cSt) | | | 12cSt (from 8cSt) | | |
|---------|--|-------|-------|------------------|-------|-------|--------------------|-------|-------|-------------------|-------|-------|
| Polymer | Characteristic Droplet Sizes (µm) @9ml/min | | | | | | | | | | | |
| | Aero. | Mist | Spray | Aero. | Mist | Spray | Aero. | Mist | Spray | Aero. | Mist | Spray |
| 95% CI | ± 2.4 | ± 8.2 | ± 18 | ± 2.4 | ± 8.2 | ± 18 | ± 2.4 | ± 8.2 | ± 18 | ± 2.4 | ± 8.2 | ± 18 |
| 1 | - | - | 460 | 11 | 83 | 630 | - | - | - | - | - | 184 |
| 2 | | | | - | 46 | 540 | 15 | 73 | 540 | - | 73 | 540 |
| 3 | | | | 4.6 | - | 460 | 0.3 | 85 | 600 | 0.6, 10 | - | 540 |
| 4 | | | | 0.5 | 73 | 400 | - | - | 540 | 0.7 | 40 | 540 |
| 5 | | | | 0.6, 11 | - | 460 | 18 | 85 | 600 | - | 5.4 | 540 |
| 6 | | | | 7.4 | 40 | 340 | 0.6, 10 | - | 540 | - | 54 | 630 |
| 7 | | | | 4.6 | - | 540 | 0.3 | - | 630 | - | - | 540 |
| | Droplet Size Volume Proportions (%) @9ml/min | | | | | | | | | | | |
| | Aero. | Mist | Spray | Aero. | Mist | Spray | Aero. | Mist | Spray | Aero. | Mist | Spray |
| 95% CI | ± 0.5 | ± 2.6 | ± 2.8 | ± 0.5 | ± 2.6 | ± 2.8 | ± 0.5 | ± 2.6 | ± 2.8 | ± 0.5 | ± 2.6 | ± 2.8 |
| 1 | - | - | 100.0 | 6.1 | 20.0 | 73.9 | - | - | - | - | 0.0 | 100.0 |
| 2 | | | | - | 2.2 | 97.8 | 0.5 | 1.0 | 98.6 | - | 1.2 | 98.8 |
| 3 | | | | 0.9 | 4.2 | 94.9 | 0.1 | 3.7 | 96.2 | 1.6 | - | 98.4 |
| 4 | | | | 0.6 | 3.6 | 95.7 | - | 6.4 | 93.6 | 0.2 | 3.4 | 96.4 |
| 5 | | | | 1.3 | - | 98.7 | 0.6 | 4.0 | 95.4 | 0.4 | - | 99.6 |
| 6 | | | | 1.3 | 6.4 | 92.4 | 1.6 | - | 98.4 | - | 1.9 | 98.1 |
| 7 | | | | 2.8 | - | 97.2 | 0.0 | - | 100.0 | - | 1.4 | 98.6 |

95% CI denotes the statistical confidence interval, some distributions have two characteristic sizes in a range (separated by commas)

conditions, the 8cSt blend of Polymer 1 produced larger droplets in mist, spray and aerosol regions versus 8cSt base oil. However, Polymer 2 did not produce mist-sized

droplets. 12cSt blends from 8cSt base oil both produced little or no aerosol compared to 12cSt blends from 4cSt base oil, Table 6.

Fig. 19 For Polymer 1; **a** variation in droplet formation tendency with lubricant inlet flow rate; **b** droplet size distributions for blends at 3 ml min^{-1} lubricant inlet flow rate (polymer concentrations in brackets)



At high flow rate, 9 ml/min, spray conditions, dramatic differences in misting tendency were observed. Polymer 1 blends had misting tendencies factors of 3 to 11 lower than equivalent Polymer 2 blends, Table 7. None of these blends were semi-dilute (no significant intermolecular interaction), suggesting viscoelasticity differences as a root cause.

Merely including Polymer 1 appeared to define behaviour. Polymer 2 showed some base oil and concentration dependency: At 3 ml/min the 12cSt blend from 4cSt base oil produced larger mist droplets ($63 \mu\text{m}$ vs. $40 \mu\text{m}$) but greater proportion of aerosol (5.8% vs. 0%) versus 12cSt blend from 8cSt base oil.

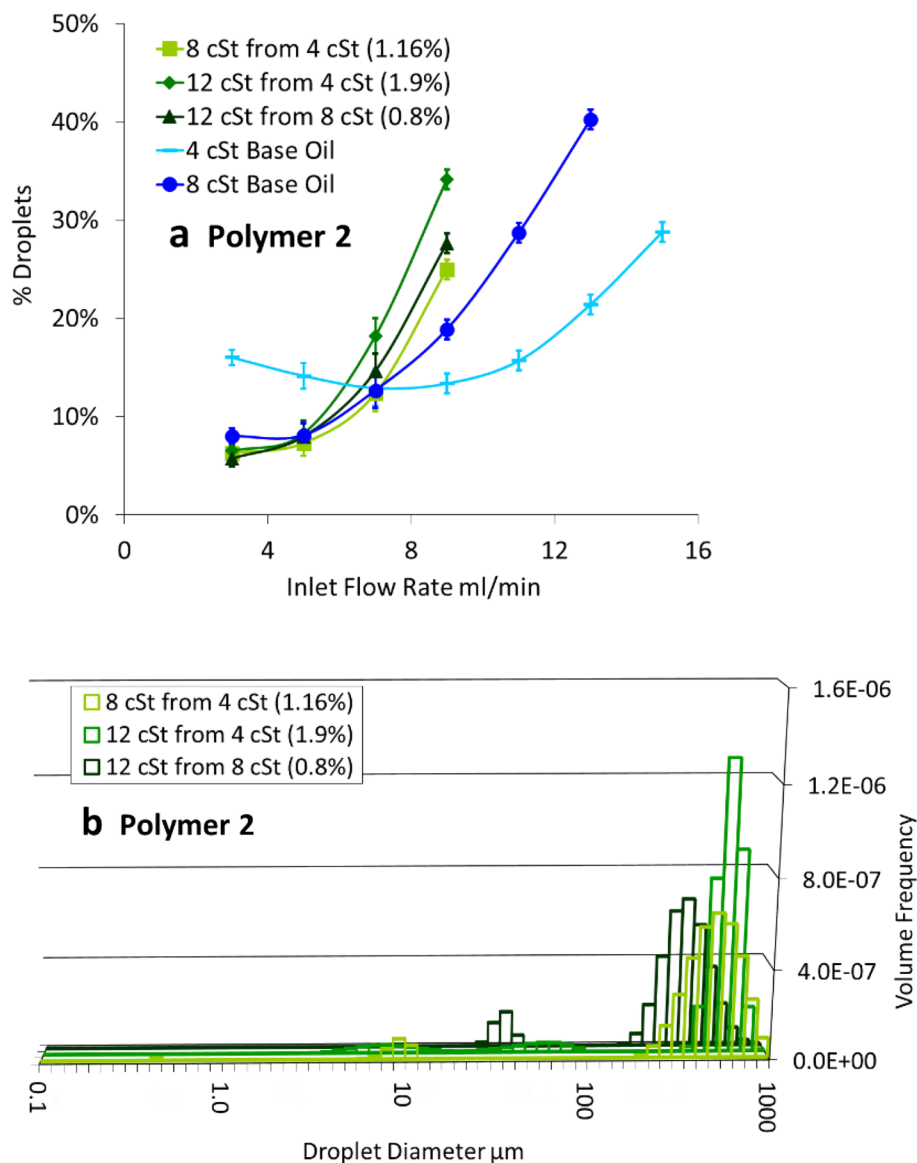
7.4 Differences Between Long-Chain and Short-Chain OCPs: Polymers 2 and 3

Droplet formation tendency of the 8cSt Polymer 3 blend, short-chain OCP, was not significantly different to 8cSt base

oil—But was significantly lower using Polymer 2, a long chain OCP. A low concentration of long-chain molecules more effectively reduced droplet formation than a high concentration of short-chain molecules. Polymer 3 reduced aerosol formation and generally increased characteristic diameters of droplets formed, when compared to 8cSt base oil. Higher potential energy storage under extension in Polymer 2 effectively reduced mist and aerosol-sized droplet formation, and, thus, overall misting tendency.

It was possible to get similar viscometrics but substantially different misting tendency, caused by viscoelastic differences. This was particularly clear at high flow rates, spray conditions, where Polymer 3 blends had significantly lower droplet formation tendency and greater projected abscissa intercept than the equivalent Polymer 2 blend, i.e. lower resistance to shear and extension. Because short chain molecules were easily reaped (dissociated) and aligned with the shear axis, resistance to shear and extension was lower.

Fig. 20 For Polymer 2; **a** Variation in droplet formation tendency with lubricant inlet flow rate; **b** droplet size distributions for blends at 3 ml min^{-1} lubricant inlet flow rate (polymer concentrations in brackets)



Polymer 3 blends produced higher aerosol and mist proportion than equivalent Polymer 2 blends (1.6–5.2% vs. 1.2–2.2%), Table 8. The lower droplet formation influence of Polymer 3 produced greater difference in mist and aerosol formation between the two 12cSt blends using different base oils. Lower mist proportion was formed in 8cSt base oil blends. Little difference in characteristic droplet diameters and proportions between the two 12cSt blends was observed in Polymer 2 blends, indicating greater dependence on polymer properties.

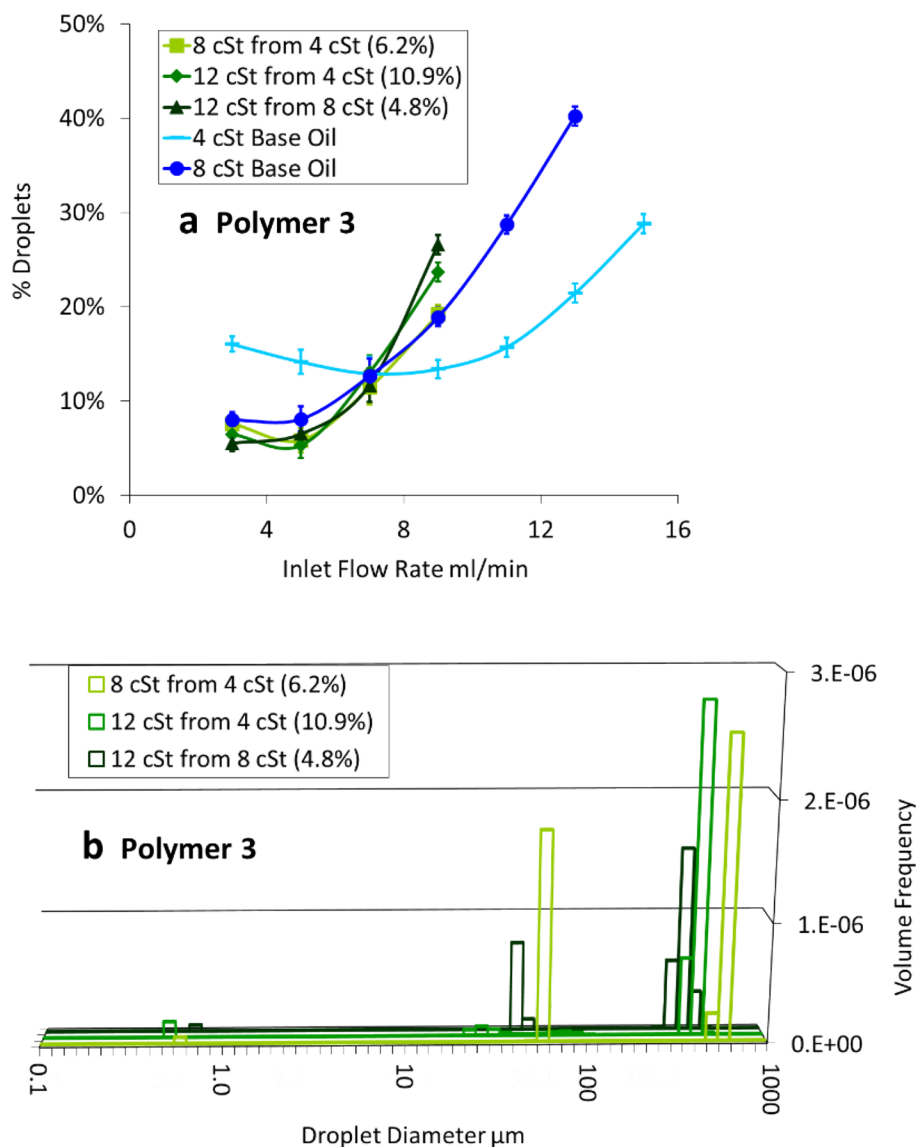
7.5 Olefin Copolymer and Styrene Butadiene: Polymers 2 and 4

Polymer 2, a high molecular weight OCP, and Polymer 4, a high molecular weight styrene-butadiene are linear

polymers. However, larger side groups and differences in base oil interaction meant styrene butadiene molecules did not coil as highly under low shear, indicated by lower self-concentration. Because Polymer 4 had greater chain length and hydrodynamic volume, a lower concentration was required to achieve blend viscosity than Polymer 2. Therefore, Polymer 2 blends had greater total capacity for energy dissipation in extension, shear and reptation, because each molecule had greater extension capacity and there were more molecules in the blend.

At low flow rate, 3 ml/min , misting conditions, both polymers reduced mist-sized droplet formation in 8cSt blends. Polymer 4 blends generated high aerosol proportions in the 8cSt blend (16.3%) and 12cSt blends (7.3–9.4%), implying lower influence on energy dissipation in shear and extension, Table 6. Thus, energy dissipation in extension depended less

Fig. 21 For Polymer 3; **a** variation in droplet formation tendency with lubricant inlet flow rate; **b** droplet size distributions for blends at 3 ml min^{-1} lubricant inlet flow rate (polymer concentrations in brackets)



on chain length (Polymer 4=4605, Polymer 2=2161) and more on capacity for extension, indicated by coiling and self-concentration.

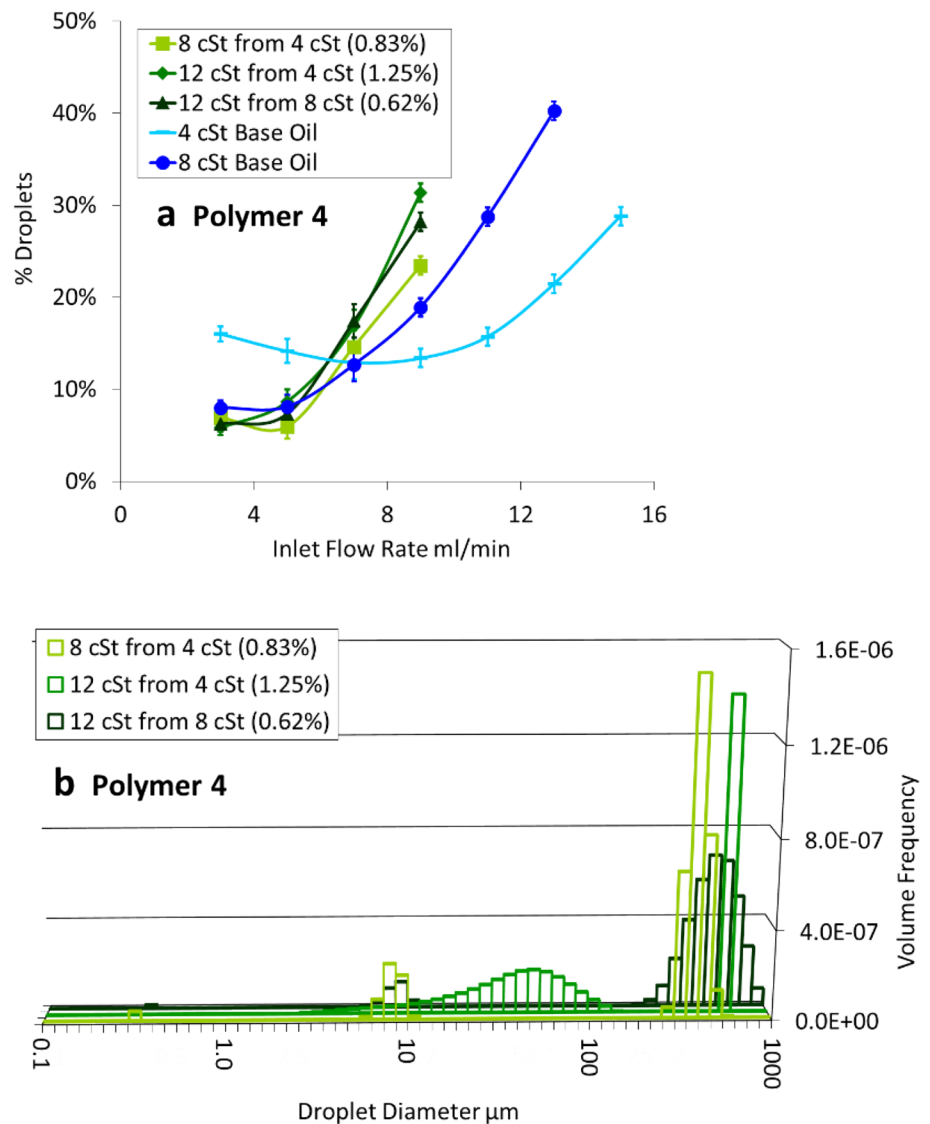
At high flow rate, 9 ml/min, spray conditions, little difference in droplet formation tendency was observed, though curves gradients were higher for Polymer 2 blends than equivalent Polymer 4 blends, Table 7. This indicates that the OCP had a greater resistance to shear and extension, i.e. greater viscoelasticity and potential energy storage. Abscissa intercepts of Polymer 4 blends decreased with increasing polymer concentration but Polymer 2 blends had the same abscissa intercept, i.e. the viscoelastic contribution of Polymer 2 was more influential than concentration. 8cSt blends of Polymers 2 and 4 were the only such blends to produce significantly higher %droplets than 8cSt base oil under these conditions. This droplet formation mechanism seemed to have high viscosity-dependency, but these

polymers increased resistance to shear and blow-through significantly. Similarly, 12cSt blends of Polymers 2 and 4 from 4cSt base oil had significantly higher gradient than all others, indicating increased resistance to shear due to viscoelasticity and, therefore, increased quantity of lubricant exposed to blow-through as flow rate increases.

7.6 Short Chain OCP and Micellar Stars: Polymers 3 and 6

Due to micellar dissociation under shear, both polymers acted, effectively, as short chain linear polymers. Arms of Polymer 6, micellar star polymer, had a chain length of 227, greater than Polymer 3 (175), a linear OCP. Dissociated, Polymer 6 arms had greater potential energy storage in extension or shear, and greater base oil solubility. Differences

Fig. 22 For Polymer 4; **a** Variation in droplet formation tendency with lubricant inlet flow rate; **b** Droplet size distributions for blends at 3 ml min^{-1} lubricant inlet flow rate (polymer concentrations in brackets)



in treat rate to produce 8cSt blends were striking: Polymer 6 = 1.46%, Polymer 3 = 6.2%.

At low flow rate, 3 ml/min, misting conditions, both polymers effectively reduced aerosol formation compared to 8cSt base oil, Table 6. The micellar star polymer produced much lower mist-sized proportion than the OCP under the same conditions. In 12cSt blends from 8cSt base oil, Polymer 6 suppressed both mist and aerosol formation but the equivalent Polymer 3 blend produced 24.9% mist-sized droplets. Both polymers produced higher mist-sized proportion in 12cSt blend from 4cSt base oil, despite higher polymer concentrations.

At high flow rate, 9 ml/min, blow-through conditions, droplet formation behaviour correlated greatest with viscosity: There were insignificant differences between the droplet formation tendency of 8cSt blends and 8cSt base oil (18.9% vs. 19.2% and 20.2% for Polymer 3 and 6, respectively),

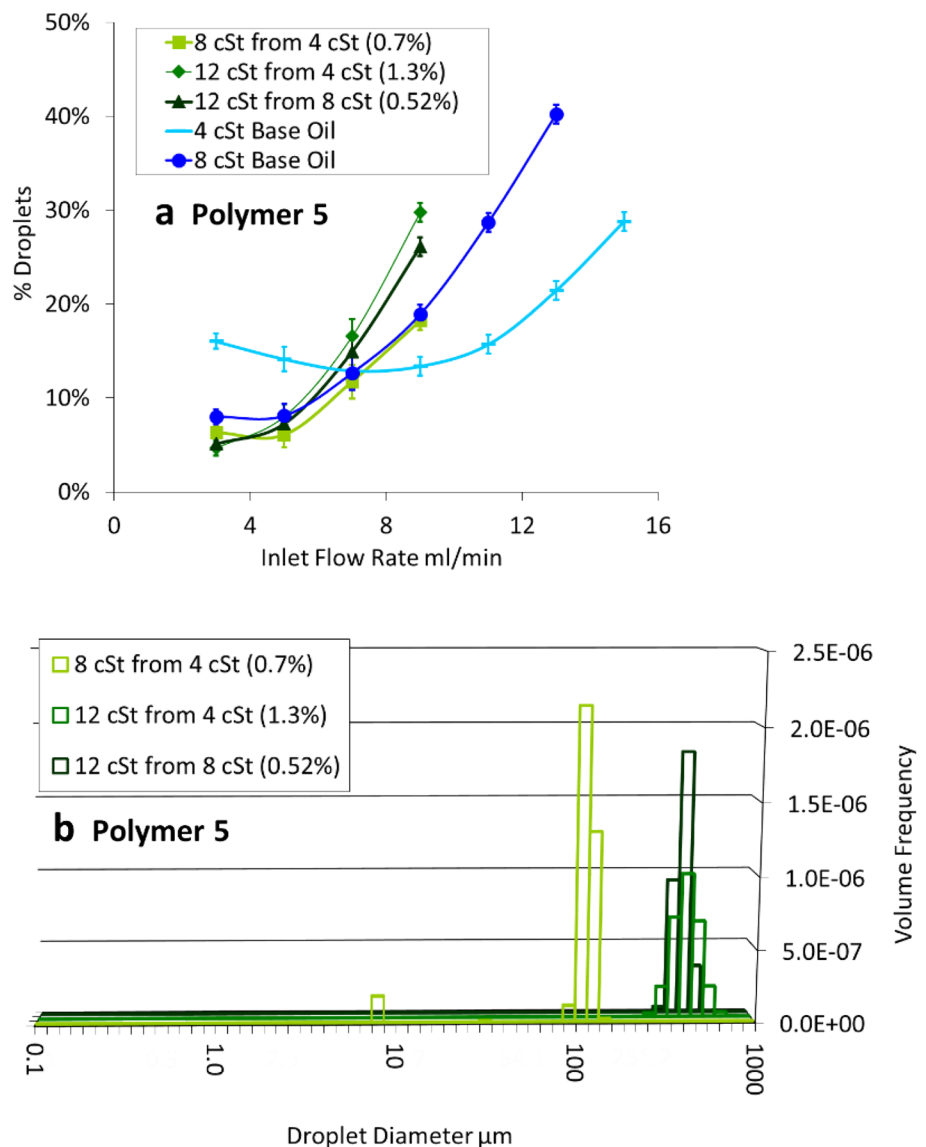
Table 7. All OCP blends produced a significant quantity of aerosol droplets: The micellar star polymer suppressed aerosol formation in the 12cSt blend from 8cSt base oil, Table 8. Overall, the micellar star polymer behaved more like a short chain OCP than a fixed star, confirming micellar dissociation under shear. The minor differences in droplet size distributions and droplet formation tendencies seemed to occur where micellar star blend curves were offset, where micelle dissociation caused variation in real viscosity.

Unlike all other 8cSt polymer blends, Polymers 3 and 6 abscissa intercepts were insignificantly different to 8cSt base oil, i.e. lower influence on resistance to droplet formation.

7.7 Base Oil Effects

In 12cSt polymer blends from 8cSt base oil, no significant difference in droplet formation tendency was observed for

Fig. 23 For Polymer 5; **a** variation in droplet formation tendency with lubricant inlet flow rate; **b** droplet size distributions for blends at 3 ml min^{-1} lubricant inlet flow rate (polymer concentrations in brackets)

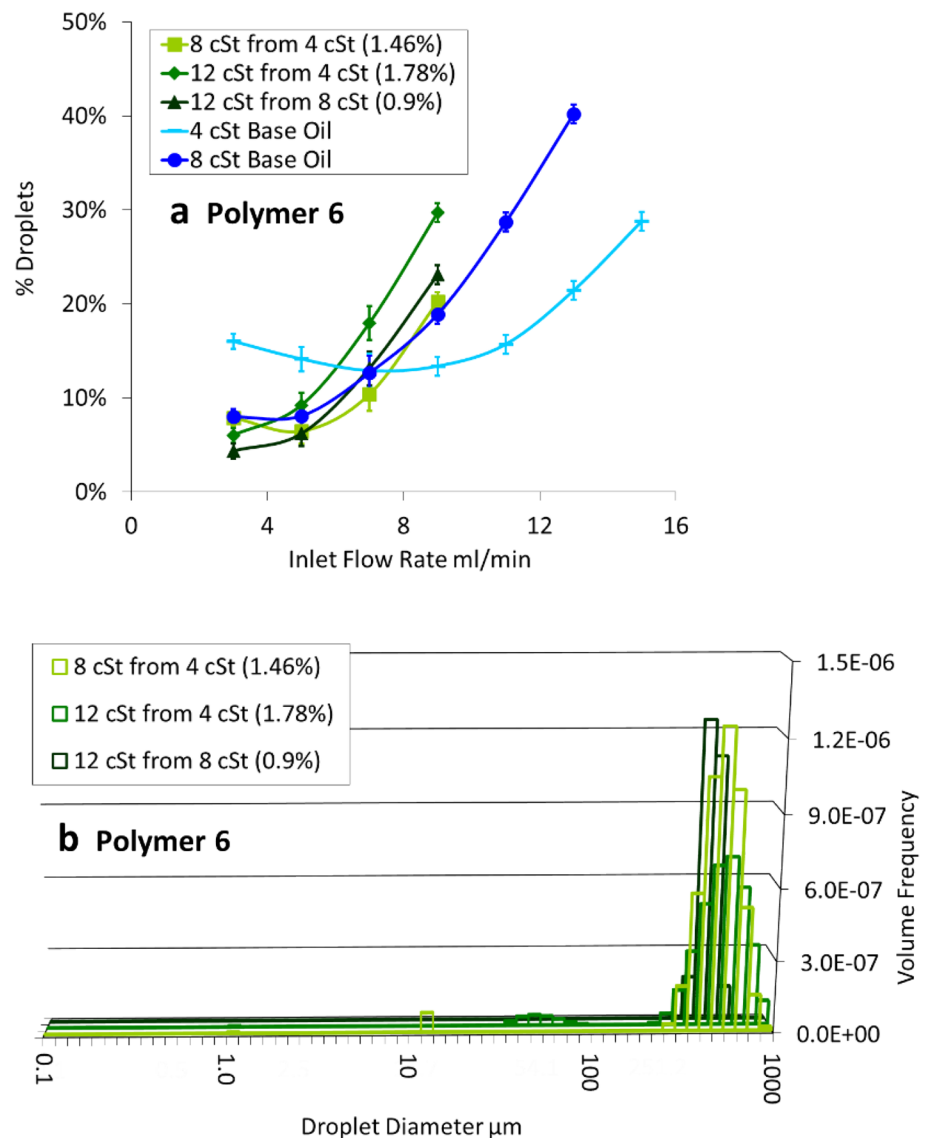


any of the polymers. This suggested that the higher viscosity base oil had a greater effect on behaviour than when a lower viscosity base oil or higher polymer content was used. In many blends, the polymer content of the 12cSt blends in 8cSt base oil was of similar magnitude to 8cSt blends from 4cSt base oil: The droplet formation of lubricants with lower viscosity base oils were more sensitive to the polymers they contained. This is logical, as lower viscosity base oils have a higher droplet formation tendency, Fig. 8.

8 Concluding Remarks on the Detailed Consideration of Viscosity Modifiers

- The tendency of polymers to reduce droplet formation was dependent on the storage of shear energy elastically in the stretching and bending of the molecule.
- The representative blends studied were found to be dilute or semi-dilute, thus did not indicate large-scale intermolecular interaction, though some interaction was predicted to occur in semi-dilute blends. Further work would be required to characterise behaviour at higher temperature, when molecules are more extended under zero shear conditions than at low temperature.
- Measurement of linear viscoelasticity did not correlate significantly with droplet formation behaviour for these blends. Extensional viscoelasticity may be a better predictor of droplet formation behaviour.
- The clearest explanation of droplet formation behaviour was from measuring polymer molecule size, indication of coiling and potential to store energy in bending, shear and extension [55].
- Linear polymers had the greatest capacity to store energy under shear and extension. Therefore, typically,

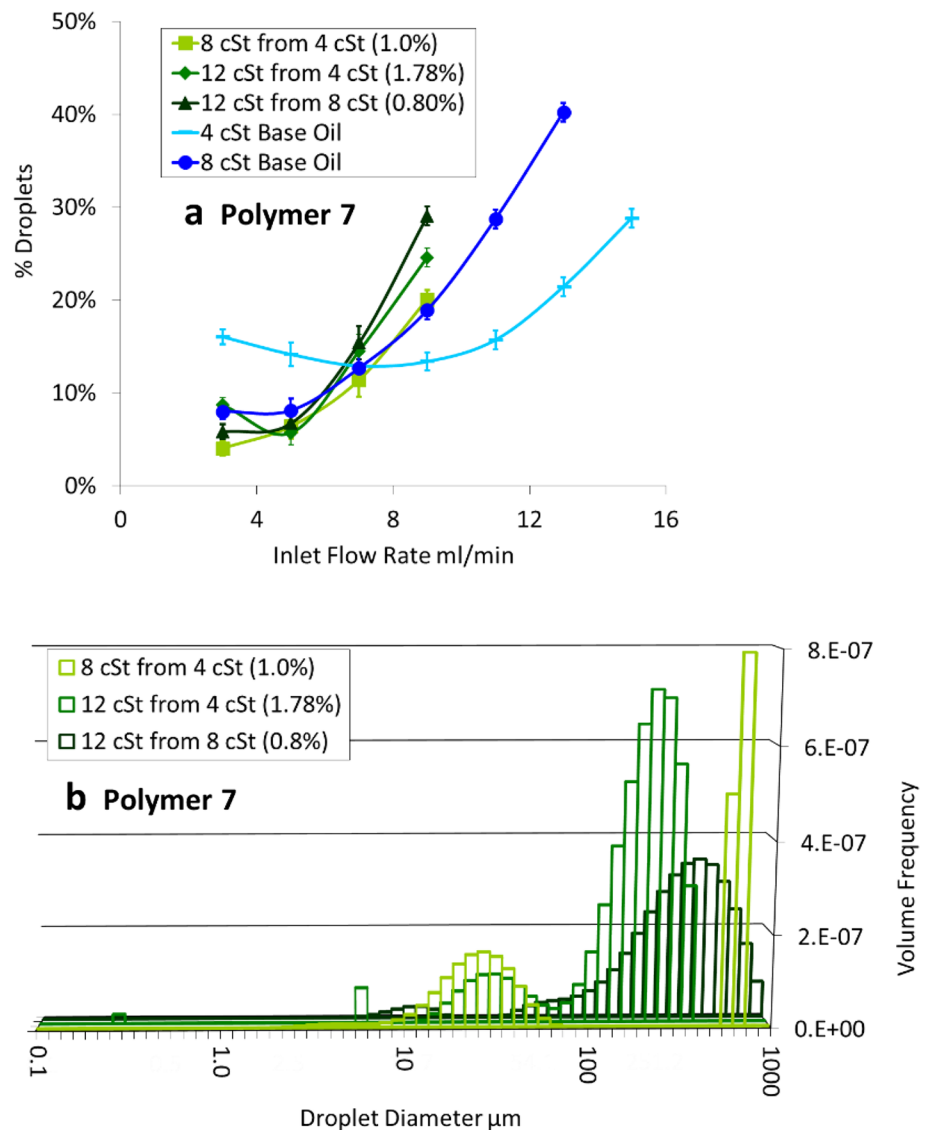
Fig. 24 For Polymer 6; **a** variation in droplet formation tendency with lubricant inlet flow rate; **b** droplet size distributions for blends at 3 ml min^{-1} lubricant inlet flow rate (polymer concentrations in brackets)



linear polymer blends most greatly reduced droplet formation. The concentration of long chain linear polymers had a great effect on droplet formation tendency. However, in some blends, the mere presence of the polymer at a significant concentration defined droplet formation.

- Storage of energy in linear polymers depended on ability to extend and uncoil. Therefore, styrene-butadiene had lower effect than olefin copolymers: Their more hindered structure and greater base oil solubility restricted coiling, and, thus, potential for energy storage.
- Below a certain molecular weight, linear polymers had reduced effect on droplet formation. Short chains did not readily coil and were easily extended. In these blends, droplet formation primarily depended on blend viscosity. Low reduction in droplet formation was further indicated by the high aerosol proportions formed by these blends.
- In fixed star polymer blends, hindered bending and limited extension of the molecules meant misting tendency reduction was less significant than for linear polymers: Less energy could be stored in a molecule. Misting tendency of star polymer blends depended more greatly on blend viscosity rather than polymer concentration.
- Micellar star polymers dissociated readily under shear. As individual arms, behaviour was similar to short chain linear polymers where little reduction in misting tendency was seen and variation depended on blend viscosity rather than polymer concentration. Behaviour was also affected by changes in viscosity induced by micellar dissociation, altering the effective architecture of the polymers and their thickening effect.
- Further work on defining the extensional viscometrics and viscoelasticity of different polymers in lubricants, and the quantity of energy that can be stored in polymer

Fig. 25 For Polymer 7; **a** variation in droplet formation tendency with lubricant inlet flow rate; **b** droplet size distributions for blends at 3 ml min^{-1} lubricant inlet flow rate (polymer concentrations in brackets)



molecules with varying architectures, would allow further quantification of these phenomena.

9 Implications for Industry

Lower viscosity oils and API Group IV synthetic base oils, rather than the refined oils of API Groups I–III, have shown an increased tendency to form droplets in this research. This observation has important implications for the transport and health of a lubricant in a modern engine. As industry moves towards lower viscosity lubricants to reduce friction power loss and API Group IV base oils for increased lubricant life, the tendency for these lubricants to form droplets will increase. Positively, increased droplet flow may mean increased availability of lubricant in critical regions of the engine, e.g. the top piston ring zone, especially during

start-up of the engine. Of greater concern, greater droplet transport in gas flows may result cause increased lubricant consumption and hydrocarbon exhaust emissions as more lubricant may reach the combustion chamber via either the top piston land or gas recirculation: This has shown to affect combustion by causing Low Speed Pre-Ignition (LSPI) [3–7]. The burden on gas filters, for example crankcase breathers, is likely to increase too, as more droplets require filtration.

Balancing this, modern engine oils of low viscosity and synthetic base oils generally require significant quantities of viscosity modifier additive to achieve a specific SAE multi-grade engine oil specification and thereby maintain acceptable viscosity over a wide temperature range. So, the effect of low viscosity and synthetic base oil in increasing the tendency to form droplets will be countered by the viscosity modifier. This research has therefore clearly shown that there

is another dimension to consider in the already complex and delicate lubricant formulation process, especially when essential surface-active additives (detergents, dispersant and antifoam) have been shown to increase droplet formation.

Hybrid engines will experience more intermittent operation and more frequent sudden transient events, e.g. starting at high speed [40]: As reported by Przesmitzki and Tian [24], blow-through oil transport mechanisms are linked to transient events, i.e. this mechanism could be more influential in hybrid engines. As reported by Taylor [40], hybrid engines also tend to experience lower oil temperatures and greater fuel dilution than conventional engines, both of which are likely to affect the viscometry and viscoelasticity of the lubricant and, thus, the droplet formation tendency.

There is the potential to produce polymer-containing lubricant blends with similar viscosities and viscosity indices but significantly different tendencies to form droplets and different sizes of droplet, by utilising different polymer architectures and different degrees of interaction between molecules under shear. There is potential to vary droplet formation tendency and viscosity somewhat independently. Through this, the flows of lubricant through various systems in an automotive engine, especially the piston assembly, may be optimised.

The droplet formation tendencies of lubricants formulated from lower viscosity base oils were more sensitive to the effect of polymers than those using higher viscosity base oils. This is logical as lower viscosity base oils themselves have a greater droplet formation tendency. However, it should not be assumed that the blend performance is a superimposition of the polymer behaviour and the base oil behaviour—Performance was clearly affected by the interaction between the polymer and base oil too. Therefore, as lower viscosity lubricants become increasingly commonplace, increasing sensitivity to the type and concentration of viscosity modifier may necessitate greater consideration for formulators, especially regarding droplet formation.

10 Conclusions

1. An experimental rig was developed to generate and characterise oil mist flows considered representative of those produced at the top piston ring gap of an automotive engine. Importantly, this involved constraining the inlet oil flow rate below a critical value, for a particular oil viscosity, to ensure a rolling droplet formation that yielded smaller droplet sizes.
2. The tendency of four API Group IV base oils, PAOs, to form mist decreased linearly with increasing average molecular weight and decreased as a third order polynomial with increasing dynamic viscosity.

3. There was no significant difference in misting tendency observed between refined mineral oils of different API Groups (I-III) and of similar viscosity, despite their different molecular weight distributions. However, an API Group IV polyalphaolefin of similar viscosity showed significantly greater tendency to produce droplets, presumably due its different molecular structure.
4. A fully formulated lubricant had a lower misting tendency than the base oil on which it was formulated. When commercial additives were included individually in the base oil, the viscosity modifier was shown to be the major factor causing this reduction in misting tendency.
5. Detailed consideration of different viscosity modifier architectures showed that the influence of the polymer molecules on the viscoelasticity of the lubricant was the mechanism that caused this.
6. In particular, high molecular weight linear polymers had the greatest tendency to reduce droplet formation: More so than star polymers.
7. Analysis of the polymer molecules indicated that the viscoelastic response was influenced by the capacity of the molecule to extend: This was indicated by self-concentration and hydrodynamic volume.
8. The results of this research have demonstrated that the selection process for base oils and functional additives in automotive engine lubricant formulations needs to also consider the tendency to form oil mist alongside all the other functions and behaviours of the fully formulated lubricant.

Acknowledgements Many thanks to the EPSRC Equipment Loan Pool for access to the laser diffraction particle sizer. The authors also wish to acknowledge the expert suggestions and feedback from Professor R C Coy whilst he was a visiting professor at the University of Leeds, UK

Declarations

Conflict of interest The authors have no relevant financial or non-financial interests to disclose.

Open Access This article is licensed under a Creative Commons Attribution 4.0 International License, which permits use, sharing, adaptation, distribution and reproduction in any medium or format, as long as you give appropriate credit to the original author(s) and the source, provide a link to the Creative Commons licence, and indicate if changes were made. The images or other third party material in this article are included in the article's Creative Commons licence, unless indicated otherwise in a credit line to the material. If material is not included in the article's Creative Commons licence and your intended use is not permitted by statutory regulation or exceeds the permitted use, you will need to obtain permission directly from the copyright holder. To view a copy of this licence, visit <http://creativecommons.org/licenses/by/4.0/>.

References

- Mufti, R.A., Priest, M.: Effect of engine operating conditions and lubricant rheology on the distribution of losses in an internal combustion engine. *Trans. ASME J. Tribol.* **131**(041101), 1–9 (2009)
- Tung, S.C., McMillan, M.: Automotive tribology overview of current advances and challenges for the future. *Tribol. Int.* **37**, 517–536 (2004)
- Dahnz, C., Han, K.-M., Spicher, U., Magar, M., Schiessl, R., Maas, U.: Investigations on pre-ignition in highly supercharged SI engines. SAE Technical Paper 2010-01-0355 (2010).
- Fletcher, K.A., Dingwell, L., Yang, K., Lam, W.Y., Styer, J.P.: Engine oil additive impacts on low speed pre-ignition. SAE Technical Paper 2016-01-2277 (2016).
- Hu, T., Teng, H., Luo, X., Lu, C., Luo, J.: Influence of fuel dilution of crankcase oil on ignitability of oil particles in a highly boosted gasoline direct injection engine. SAE Technical Paper 2015-01-2811 (2015).
- Kassai, M., Torii, K., Shiraishi, T., Nada, T., Goh, T.K., Wilbrand, K., Wakefield, S., Healy, A., Doyle, D., Cracknell, R., Shibuya, M.: Research on the effect of lubricant oil and fuel properties on LSPI occurrence in boosted S.I. engines. SAE Technical Paper 2016-01-2292 (2016).
- Ritchie, A., Boese, D., Young, A.W.: Controlling low-speed pre-ignition in modern automotive equipment part 3: identification of key additive component types and other lubricant composition effects on low-speed pre-ignition. SAE Technical Paper 2016-01-0717 (2016).
- Brown, M.A., McCann, H., Thompson, D.M.: SAE Technical Paper 932784 (1993).
- Yasutomi, S., Maeda, Y., Maeda, T.: Kinetic approach to engine oil: 1, analysis of lubricant transport and degradation in engine system. *Ind. Eng. Chem. Prod. Res. Dev.* **20**, 530–536 (1981)
- Burnett, P.J.: SAE Technical Paper 920089 (1992).
- DePetris, C., Giglio, V., Police, G.: SAE Technical Paper 961216 (1996).
- Gamble, R.J.: PhD Thesis, University of Leeds, UK (2003).
- McGeehan, J.A.: A survey of the mechanical design factors affecting engine oil consumption. SAE Technical Paper 790864 (1979).
- Taylor, R.I., Evans, P.G.: In-situ piston measurements. *Proc. IMechE* **218**, 185–200 (2004)
- Thirouard, B., Tian, T., Hart, D.P.: Investigation of oil transport mechanisms in the piston ring pack of a single cylinder diesel engine, using two dimensional laser induced fluorescence. SAE Technical Paper 982658 (1998).
- Wannatong, K., Chanchaona, S., Sanitjai, S.: Simulation algorithm for piston ring dynamics. *Simul. Modell. Theory Pract.* **16**, 127–146 (2008)
- Wong, V.W., Thomas, B.C., Watson, S.A.G.: Bridging Macroscopic Lubricant Transport and Surface Tribochemical Investigations in Reciprocating Engines. *Proceedings of the IMechE: J Journal of Engineering Tribology* **221**, 183–193 (2007)
- Yilmaz, E., Tian, T., Wong, V.W., Heywood, J.B.: The contribution of different oil consumption sources to total oil consumption in a spark ignition engine. SAE Technical Paper 2004-01-2909 (2004).
- Audette-III, W. A., Wong, V.: Oil transport along the engine cylinder liner: coupling vaporization and film-thickness analysis. In: 12th International Colloquium Tribology 2000-Plus, Technische Akademie Esslingen, Ostfildern, Germany, January 11–13, 2000
- Furuhama, S., Takiguchi, M., Tomizawa, K.: Effect of piston and piston ring designs on the piston friction forces in diesel engines. SAE Technical Paper 810977 (1981).
- Guenther, M., DeWaard, D., LaPan, M., Jensen, T., Seigl, W., Baldus, S., Loo, J.: Comparison of vehicle running loss evaporative emissions using point source and enclosure measurement techniques. SAE Technical Paper 980403 (1998).
- Tatli, E., Clark, N.N.: Crankcase particulate emissions from diesel engines. SAE Technical Paper 2008-01-1751 (2008).
- Yilmaz, E., Tian, T., Wong, V.W., Heywood, J.B.: An experimental and theoretical study of the contribution of oil evaporation to oil consumption. SAE Technical Paper 2002-01-2684 (2002).
- Przesmitzki, S., Tian, T., Oil transport inside the power cylinder during transient load changes. SAE Technical Paper 2007-01-1054 (2007).
- Tian, T.: Dynamic behaviours of piston rings and their practical impact: part 1, ring flutter and ring collapse and their effects on gas flow and oil transport. *Proc. IMechE J.* **216**, 209–227 (2002)
- Ito, A., Tsuchihashi, K., Nakamura, M.: A study on the mechanism of lubricating oil consumption of diesel engines - 4th report: the measurement of oil pressure under the piston oil ring. SAE Technical Paper 2006-01-3440 (2006).
- McGrogan, S., Tian, T.: Numerical simulation of combustion-driven oil transport on the top land of an internal combustion engine. *Int. J. Engine Res.* **11**, 243–256 (2010)
- Gamble, R.J., Priest, M., Taylor, C.M.: Detailed analysis of oil transport in the piston assembly of a gasoline engine. *Tribol. Lett.* **14**, 147–156 (2002)
- Gulwadi, S.D.: A mixed lubrication and oil transport model for piston rings using a mass-conserving algorithm. *Trans. ASME* **120**, 199–208 (1998)
- Ishihara, S., Nakashima, K., Urano, K., Murata, K.: SAE Technical Paper 1999-01-3316 (1999).
- Keribar, R., Dursunkaya, Z., Fleming, M.F.: An integrated model of ring pack performance. *Trans. ASME* **113**, 382–389 (1991)
- Saito, K., Igashira, T., Nakada, M.: Analysis of oil consumption by observing oil behaviour around piston ring using a glass cylinder engine. SAE Technical Paper 892107 (1989).
- Usui, M., Murayama, K., Oogake, K., Yoshida, H., SAE Technical Paper 2008-01-0795 (2008).
- Min, B.-S., Kim, J.-S., Oh, D.-Y., Choi, J.-K., Jin, J.-H.: SAE Technical Paper 982442 (1998).
- Nakashima, K., Ishihara, S., Urano, K.: SAE Technical Paper 952546 (1995).
- Cho, Y., Tian, T.: Modeling engine oil vaporization and transport of the oil vapor in the piston ring pack of internal combustion engines. SAE Technical Paper 2004-01-2912 (2004).
- Day, L., Dunaevsky, V., McCormick, H.: Critical factors affecting oil consumption and deposit formation in engines and compressors come to light from research in two disciplines. *Tribol. Lubr. Technol. STLE* **2008**, 31–39 (2008)
- Dasch, J.M., D'Arcy, J.B., Kinare, S.S., Yin, Y., Koppale, R.G., Salmon, S.C.: Mist Generation from High-Speed Grinding with Straight Oils. *Tribol. Trans.* **51**, 381–388 (2008)
- Uy, D., Storey, J., Sluder, C.S., Barone, T., Lewis, S., Jagner, M.: Effects of oil formulation, oil separator, and engine speed and load on the particle size, chemistry, and morphology of diesel crankcase aerosols. SAE Technical Paper 2016-01-0897 (2016).
- Taylor, R.I.: Energy efficiency, emission, tribological challenges and fluid requirements of electrified passenger cars. *Lubricants* **9** (2021)
- Williamson, B.P., Milton, A.: Characterisation of the viscoelasticity of engine lubricants at elevated temperatures and shear rates. SAE Technical Paper 951032 (1995).
- Ohtani, H., Ellwood, K., Pereira, G., Chinen, T., Selvasekar, S.: Extensional rheology: new dimension of characterizing automotive fluids. SAE Technical Paper 2017-01-0364 (2017).
- Begg, S.M., De-Sercey, G., Miche, N.D.D., Heikal, M.R., Gilchrist, R., Noda, Y., Tsuruoka, Y., Mamiya, Y.: Experimental

- investigation of the phenomenon of oil breakup in an engine crankcase. *Atomiz. Sprays* **20**, 801–819 (2010)
44. Hewitt, G.F., Hall-Taylor, N.S.: *Annular Two-Phase Flow*. Pergamon Press 1970.
 45. Marano, R.S., Messick, R.L., Smolinold, J.M., Toth, L.: SAE Technical Paper 950245 (1995).
 46. Smolinski, J.M., Gulari, E., Manke, C.W.: Atomization of dilute polyisobutylene/mineral oil solutions. *AIChE J.* **42**, 1201–1212 (1996)
 47. McKinley, G.H.: Dimensionless groups for understanding free surface flows of complex fluids. *SOR Rheol. Bull.* (2005).
 48. Ohmori, T., Tohyama, M., Yamamoto, M., Akiyama, K., Tasaka, K., Yoshihara, T.: SAE Technical Paper 932782 (1993).
 49. Ferry, J.D.: *Viscoelastic Properties of Polymers*. Wiley, New York (1980)
 50. Graessley, W.W.: *Polymeric liquids and networks: dynamics and rheology*. Garland Science (2008)
 51. Rhodes, R. B., Star polymer viscosity index improver for oil compositions (1999).
 52. Mortier, R.M., Orszulik, S.T.: *Chemistry and Technology of Lubricants*, 3rd edn. Blackie Academic and Professional (2010).
 53. ASTM, D2270 - Standard practice for calculating viscosity index from kinematic viscosity at 40 and 100°C (2010).
 54. Schulz, D.N., Glass, J.E.: *Polymers as rheology modifiers*. In: ACS Symposium Series (1991).
 55. Willett, E., DeVore, A., Vargo, D.: Coeur d'Alene. ID, USA (2018).

Publisher's Note Springer Nature remains neutral with regard to jurisdictional claims in published maps and institutional affiliations.